

Supplemental Information for Refining siliceous zeolite framework structures with
 ^{29}Si NMR Spectroscopy

Deepansh J. Srivastava*
Hyperfine, Inc., Guilford, CT, USA

Maxwell Venetos†
Department of Materials Science and Engineering, University of California, Berkeley, CA, USA

Alexis McCarthy‡ and Philip J. Grandinetti§
*Department of Chemistry, Ohio State University,
100 West 18th Avenue, Columbus, OH 43210, USA*

Jay H. Baltisberger¶
Wacker Chemical

Darren Brouwer**
Department of Chemistry, Redeemer University, Ancaster ON, L9K 1J4, Canada

* srivastava.89@osu.edu

† mvenetos@berkeley.edu

‡ mccarthy.677@osu.edu

§ grandinetti.1@osu.edu

¶ Baltisberger@wacker.com

** dbrouwer@redeemer.ca

CONTENTS

S1. Shifted-Echo PIETA Transition and Symmetry Pathways	S2
S2. Relaxation parameter for Sigma-2 and ZSM-12	S8
S3. Single v.s. Multi SE-PIETA averaged spectra of ZSM-12	S9
S4. Bruker Pulse Sequences	S10
A. SE-PIETA with t_1 interleaving	S10
S5. Interleaved Shifted-Echo PIETA Signal Processing	S15
S6. Structure Refinements	S31
A. Optimization of Sigma-2	S31
B. Optimization of ZSM-12	S35
References	S40

S1. SHIFTED-ECHO PIETA TRANSITION AND SYMMETRY PATHWAYS

We describe the Shifted-Echo PIETA sequence using the symmetry pathway formalism[1] which generalizes the concept of coherence transfer pathways[2] to the “spatial pathway,” which maps into a set of *spatial symmetry pathways*, and the “transition pathway,” which maps into a set of *transition symmetry pathways*. In the case of weak J coupling between dilute ^{29}Si – ^{29}Si pairs under fast magic-angle spinning (MAS) the rotating frame transition frequency is given by

$$\Omega_{AX} = -\omega_0\sigma_{\text{iso},A} \wp_A - \omega_0\sigma_{\text{iso},X} \wp_X - 2\pi J_{AX} (\wp\wp)_{AX}, \quad (1)$$

where the transition symmetry functions are given by

$$\begin{aligned} \wp_A &= m_{A,j} - m_{A,i}, \\ \wp_X &= m_{X,j} - m_{X,i}, \\ (\wp\wp)_{AX} &= m_{A,j}m_{X,j} - m_{A,i}m_{X,i}. \end{aligned} \quad (2)$$

Here $\sigma_{\text{iso},A}$ and $\sigma_{\text{iso},X}$ are the isotropic nuclear shieldings, ω_0 is the Larmor frequency and J_{AX} is the indirect coupling constant. The quantum numbers, m_A and m_X , are associated with a quantized energy levels of A and X nuclei, respectively, while i and j represents the initial and final energy state of the NMR transition. The \wp_A , \wp_X , and \wp_{AX} values for single quantum transitions in a system of two weakly coupled spin 1/2 nuclei are shown in Fig. S1. In the case of two weakly coupled homonuclear nuclei it is useful to define the additional transition symmetry function $\wp_{AX} = \wp_A + \wp_X$. The \wp_A , \wp_X , and $(\wp\wp)_{AX}$ spin transition symmetry functions reflect their symmetry under the orthogonal rotation subgroup where simple rules hold under a π pulse, such as, the $(\wp\wp)_{AX}$ spin transition symmetry function is invariant, whereas, \wp_A , \wp_X and \wp_{AX} spin transition symmetry functions change sign.

This section explicitly lists all 32 detectable spin transition pathways of 2D shifted echo PIETA pulse sequence introduced by Srivastava et al.[4]. Based on the transition symmetry functions, these 32 transition pathways can be grouped into four sets of eight transition pathways. For the following eight spin transitions,

$$\begin{aligned} \frac{\pi}{2} \rightarrow A_1 \xrightarrow{\pi} A_2^* \xrightarrow{\frac{\pi}{2}} X_1^* \left[\xrightarrow{\pi} X_2(t_1) \xrightarrow{\pi} X_1^* \right]_{\kappa}, \\ \frac{\pi}{2} \rightarrow A_2 \xrightarrow{\pi} A_1^* \xrightarrow{\frac{\pi}{2}} X_2^* \left[\xrightarrow{\pi} X_1(t_1) \xrightarrow{\pi} X_2^* \right]_{\kappa}, \end{aligned} \quad (\text{P.1})$$

$$\begin{aligned} \frac{\pi}{2} \rightarrow X_1 \xrightarrow{\pi} X_2^* \xrightarrow{\frac{\pi}{2}} A_1^* \left[\xrightarrow{\pi} A_2(t_1) \xrightarrow{\pi} A_1^* \right]_{\kappa}, \\ \frac{\pi}{2} \rightarrow X_2 \xrightarrow{\pi} X_1^* \xrightarrow{\frac{\pi}{2}} A_2^* \left[\xrightarrow{\pi} A_1(t_1) \xrightarrow{\pi} A_2^* \right]_{\kappa}, \end{aligned} \quad (\text{P.2})$$

$$\begin{aligned} \frac{\pi}{2} \rightarrow A_1 \xrightarrow{\pi} A_2^* \xrightarrow{\frac{\pi}{2}} A_1^* \left[\xrightarrow{\pi} A_2(t_1) \xrightarrow{\pi} A_1^* \right]_{\kappa}, \\ \frac{\pi}{2} \rightarrow A_2 \xrightarrow{\pi} A_1^* \xrightarrow{\frac{\pi}{2}} A_2^* \left[\xrightarrow{\pi} A_1(t_1) \xrightarrow{\pi} A_2^* \right]_{\kappa}, \end{aligned} \quad (\text{P.3})$$

$$\begin{aligned} \frac{\pi}{2} \rightarrow X_1 \xrightarrow{\pi} X_2^* \xrightarrow{\frac{\pi}{2}} X_1^* \left[\xrightarrow{\pi} X_2(t_1) \xrightarrow{\pi} X_1^* \right]_{\kappa}, \\ \frac{\pi}{2} \rightarrow X_2 \xrightarrow{\pi} X_1^* \xrightarrow{\frac{\pi}{2}} X_2^* \left[\xrightarrow{\pi} X_1(t_1) \xrightarrow{\pi} X_2^* \right]_{\kappa}, \end{aligned} \quad (\text{P.4})$$

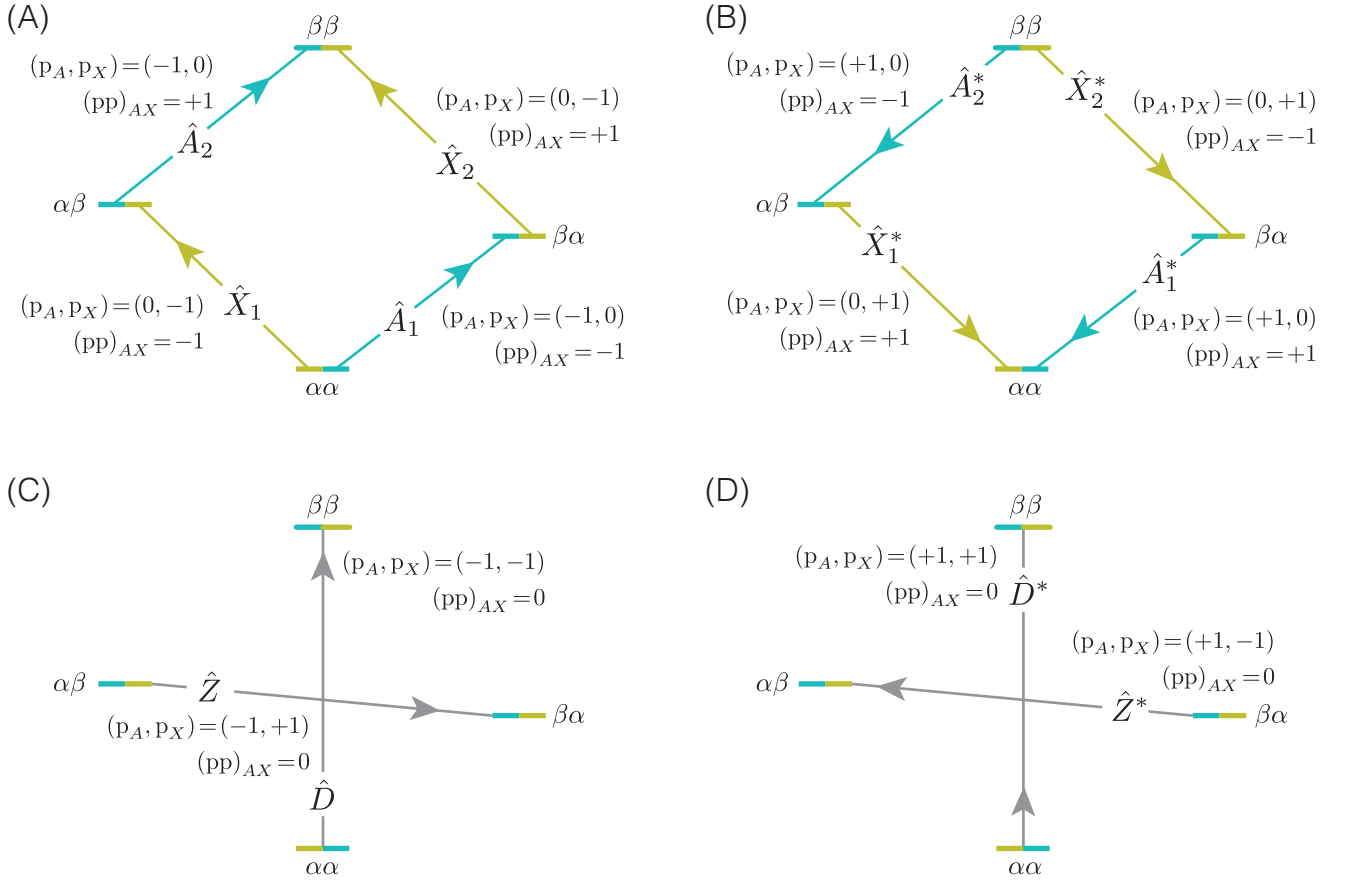


FIG. S1. Energy level diagram of two weakly coupled spin $I = 1/2$ nuclei, where $\alpha = m = +1/2$ and $\beta = m = -1/2$, with transition labeled according to their transition symmetry function values for (A) $p_{AX} = -1$ transitions, i.e., \hat{A}_1 , \hat{A}_2 , \hat{X}_1 , and \hat{X}_2 , (B) $p_{AX} = +1$ transitions, i.e., \hat{A}_1^* , \hat{A}_2^* , \hat{X}_1^* , and \hat{X}_2^* , (C) $p_{AX} = -2$ transitions, i.e., \hat{D} and \hat{Z} , and (D) $p_{AX} = +2$ transitions, i.e., \hat{D}^* and \hat{Z}^* . Note that each transition has a unique set of transition symmetry function values, p_A , p_X , and $(pp)_{AX}$. Note, that the integer-scaled transition symmetry functions,[3] $p = \wp$ and $(pp)_{AX} = 2(\wp\wp)_{AX}$ are displayed in the figure.

the associated spin transition symmetry pathways are

$$\begin{aligned} \wp_{AX} = 0 &\xrightarrow{\frac{\pi}{2}} -1 \xrightarrow{\pi} +1 \xrightarrow{\frac{\pi}{2}} +1 \left[\xrightarrow{\pi} -1(t_1) \xrightarrow{\pi} +1 \right]_{\kappa}, \\ 2(\wp\wp)_{AX} = 0 &\xrightarrow{\frac{\pi}{2}} \mp 1 \xrightarrow{\pi} \mp 1 \xrightarrow{\frac{\pi}{2}} \pm 1 \left[\xrightarrow{\pi} \pm 1(t_1) \xrightarrow{\pi} \pm 1 \right]_{\kappa}. \end{aligned} \quad (\text{SP.1})$$

This is the set of pathways for the odd-numbered echoes having an accumulated value of $\Delta p_1 = +3$ in the pulse sequence with the RF phase of the first three pulses defined in terms of ϕ_1 with every other π pulse phase set to ϕ_2 in the echo train acquisition, as shown in Fig. S2.

The next group of eight spin transition pathways,

$$\begin{aligned} \frac{\pi}{2} \rightarrow A_1^* \xrightarrow{\pi} A_2 \xrightarrow{\frac{\pi}{2}} X_1 \left[\xrightarrow{\pi} X_2^* \xrightarrow{\pi} X_1(t_1) \right]_{\kappa}, \\ \frac{\pi}{2} \rightarrow A_2^* \xrightarrow{\pi} A_1 \xrightarrow{\frac{\pi}{2}} X_2 \left[\xrightarrow{\pi} X_1^* \xrightarrow{\pi} X_2(t_1) \right]_{\kappa}, \end{aligned} \quad (\text{P.9})$$

$$\begin{aligned} \frac{\pi}{2} \rightarrow X_1^* \xrightarrow{\pi} X_2 \xrightarrow{\frac{\pi}{2}} A_1 \left[\xrightarrow{\pi} A_2^* \xrightarrow{\pi} A_1(t_1) \right]_{\kappa}, \\ \frac{\pi}{2} \rightarrow X_2^* \xrightarrow{\pi} X_1 \xrightarrow{\frac{\pi}{2}} A_2 \left[\xrightarrow{\pi} A_1^* \xrightarrow{\pi} A_2(t_1) \right]_{\kappa}, \end{aligned} \quad (\text{P.10})$$

$$\begin{aligned} \frac{\pi}{2} \rightarrow A_1^* \xrightarrow{\pi} A_2 \xrightarrow{\frac{\pi}{2}} A_1 \left[\xrightarrow{\pi} A_2^* \xrightarrow{\pi} A_1(t_1) \right]_{\kappa}, \\ \frac{\pi}{2} \rightarrow A_2^* \xrightarrow{\pi} A_1 \xrightarrow{\frac{\pi}{2}} A_2 \left[\xrightarrow{\pi} A_1^* \xrightarrow{\pi} A_2(t_1) \right]_{\kappa}, \end{aligned} \quad (\text{P.11})$$

$$\begin{aligned} \frac{\pi}{2} \rightarrow X_1^* \xrightarrow{\pi} X_2 \xrightarrow{\frac{\pi}{2}} X_1 \left[\xrightarrow{\pi} X_2^* \xrightarrow{\pi} X_1(t_1) \right]_{\kappa}, \\ \frac{\pi}{2} \rightarrow X_2^* \xrightarrow{\pi} X_1 \xrightarrow{\frac{\pi}{2}} X_2 \left[\xrightarrow{\pi} X_1^* \xrightarrow{\pi} X_2(t_1) \right]_{\kappa}, \end{aligned} \quad (\text{P.12})$$

are associated with the spin transition symmetry pathways

$$\begin{aligned} \wp_{AX} = 0 \xrightarrow{\frac{\pi}{2}} +1 \xrightarrow{\pi} -1 \xrightarrow{\frac{\pi}{2}} -1 \left[\xrightarrow{\pi} +1 \xrightarrow{\pi} -1(t_1) \right]_{\kappa}, \\ 2(\wp\wp)_{AX} = 0 \xrightarrow{\frac{\pi}{2}} \mp 1 \xrightarrow{\pi} \mp 1 \xrightarrow{\frac{\pi}{2}} \pm 1 \left[\xrightarrow{\pi} \pm 1 \xrightarrow{\pi} \pm 1(t_1) \right]_{\kappa}. \end{aligned} \quad (\text{SP.2})$$

This is the set of pathways for the even-numbered echoes having an accumulated value of $\Delta p_1 = -3$ in the pulse sequence with the RF phase of the first three pulses defined in terms of ϕ_1 with every other π pulse phase set to ϕ_2 in the echo train acquisition, as shown in Fig. S2. The \wp symmetry pathways associated with the spin transition pathways in (P.9)-(P.12) are the reflection of \wp transition symmetry pathways associated with the spin transitions in (P.1)-(P.4), respectively, about the $\wp_A = \wp_X = \wp_{AX} = 0$ without reflecting $2\wp_{AX}$ transition symmetry pathway. The graphical representation of the symmetry pathways associated with the transition pathways in (P.1)-(P.4) along with the symmetry pathway, (SP.1), is shown in Fig. S2.

Similarly, for the following eight spin transition pathways,

$$\begin{aligned} \frac{\pi}{2} \rightarrow A_1^* \xrightarrow{\pi} A_2 \xrightarrow{\frac{\pi}{2}} X_2^* \left[\xrightarrow{\pi} X_1(t_1) \xrightarrow{\pi} X_2^* \right]_{\kappa}, \\ \frac{\pi}{2} \rightarrow A_2^* \xrightarrow{\pi} A_1 \xrightarrow{\frac{\pi}{2}} X_1^* \left[\xrightarrow{\pi} X_2(t_1) \xrightarrow{\pi} X_1^* \right]_{\kappa}, \end{aligned} \quad (\text{P.5})$$

$$\begin{aligned} \frac{\pi}{2} \rightarrow X_1^* \xrightarrow{\pi} X_2 \xrightarrow{\frac{\pi}{2}} A_2^* \left[\xrightarrow{\pi} A_1(t_1) \xrightarrow{\pi} A_2^* \right]_{\kappa}, \\ \frac{\pi}{2} \rightarrow X_2^* \xrightarrow{\pi} X_1 \xrightarrow{\frac{\pi}{2}} A_1^* \left[\xrightarrow{\pi} A_2(t_1) \xrightarrow{\pi} A_1^* \right]_{\kappa}, \end{aligned} \quad (\text{P.6})$$

$$\begin{aligned} \frac{\pi}{2} \rightarrow A_1^* \xrightarrow{\pi} A_2 \xrightarrow{\frac{\pi}{2}} A_2^* \left[\xrightarrow{\pi} A_1(t_1) \xrightarrow{\pi} A_2^* \right]_{\kappa}, \\ \frac{\pi}{2} \rightarrow A_2^* \xrightarrow{\pi} A_1 \xrightarrow{\frac{\pi}{2}} A_1^* \left[\xrightarrow{\pi} A_2(t_1) \xrightarrow{\pi} A_1^* \right]_{\kappa}, \end{aligned} \quad (\text{P.7})$$

$$\begin{aligned} \frac{\pi}{2} \rightarrow X_1^* \xrightarrow{\pi} X_2 \xrightarrow{\frac{\pi}{2}} X_2^* \left[\xrightarrow{\pi} X_1(t_1) \xrightarrow{\pi} X_2^* \right]_{\kappa}, \\ \frac{\pi}{2} \rightarrow X_2^* \xrightarrow{\pi} X_1 \xrightarrow{\frac{\pi}{2}} X_1^* \left[\xrightarrow{\pi} X_2(t_1) \xrightarrow{\pi} X_1^* \right]_{\kappa}, \end{aligned} \quad (\text{P.8})$$

the associated spin transition symmetry pathways are

$$\begin{aligned} \wp_{AX} = 0 \xrightarrow{\frac{\pi}{2}} +1 \xrightarrow{\pi} -1 \xrightarrow{\frac{\pi}{2}} +1 \left[\xrightarrow{\pi} -1(t_1) \xrightarrow{\pi} +1 \right]_{\kappa}, \\ 2(\wp\wp)_{AX} = 0 \xrightarrow{\frac{\pi}{2}} \mp 1 \xrightarrow{\pi} \mp 1 \xrightarrow{\frac{\pi}{2}} \pm 1 \left[\xrightarrow{\pi} \pm 1(t_1) \xrightarrow{\pi} \pm 1 \right]_{\kappa}. \end{aligned} \quad (\text{SP.3})$$

This is the set of pathways for the odd-numbered echoes having an accumulated value of $\Delta p_1 = -5$ in the pulse sequence with the RF phase of the first three pulses defined in terms of ϕ_1 with every other π pulse phase set to ϕ_2 in the echo train acquisition, as shown in Fig. S2.

The remaining eight spin transition pathways,

$$\begin{aligned} \xrightarrow{\frac{\pi}{2}} A_1 \xrightarrow{\pi} A_2^* \xrightarrow{\frac{\pi}{2}} X_2 \left[\xrightarrow{\pi} X_1^* \xrightarrow{\pi} X_2(t_1) \right]_{\kappa}, \\ \xrightarrow{\frac{\pi}{2}} A_2 \xrightarrow{\pi} A_1^* \xrightarrow{\frac{\pi}{2}} X_1 \left[\xrightarrow{\pi} X_2^* \xrightarrow{\pi} X_1(t_1) \right]_{\kappa}, \end{aligned} \quad (\text{P.13})$$

$$\begin{aligned} \xrightarrow{\frac{\pi}{2}} X_1 \xrightarrow{\pi} X_2^* \xrightarrow{\frac{\pi}{2}} A_2 \left[\xrightarrow{\pi} A_1^* \xrightarrow{\pi} A_2(t_1) \right]_{\kappa}, \\ \xrightarrow{\frac{\pi}{2}} X_2 \xrightarrow{\pi} X_1^* \xrightarrow{\frac{\pi}{2}} A_1 \left[\xrightarrow{\pi} A_2^* \xrightarrow{\pi} A_1(t_1) \right]_{\kappa}, \end{aligned} \quad (\text{P.14})$$

$$\begin{aligned} \xrightarrow{\frac{\pi}{2}} A_1 \xrightarrow{\pi} A_2^* \xrightarrow{\frac{\pi}{2}} A_2 \left[\xrightarrow{\pi} A_1^* \xrightarrow{\pi} A_2(t_1) \right]_{\kappa}, \\ \xrightarrow{\frac{\pi}{2}} A_2 \xrightarrow{\pi} A_1^* \xrightarrow{\frac{\pi}{2}} A_1 \left[\xrightarrow{\pi} A_2^* \xrightarrow{\pi} A_1(t_1) \right]_{\kappa}, \end{aligned} \quad (\text{P.15})$$

$$\begin{aligned} \xrightarrow{\frac{\pi}{2}} X_1 \xrightarrow{\pi} X_2^* \xrightarrow{\frac{\pi}{2}} X_2 \left[\xrightarrow{\pi} X_1^* \xrightarrow{\pi} X_2(t_1) \right]_{\kappa}, \\ \xrightarrow{\frac{\pi}{2}} X_2 \xrightarrow{\pi} X_1^* \xrightarrow{\frac{\pi}{2}} X_1 \left[\xrightarrow{\pi} X_2^* \xrightarrow{\pi} X_1(t_1) \right]_{\kappa}, \end{aligned} \quad (\text{P.16})$$

are associated with the spin transition symmetry pathways

$$\begin{aligned} \wp_{AX} = 0 \xrightarrow{\frac{\pi}{2}} -1 \xrightarrow{\pi} +1 \xrightarrow{\frac{\pi}{2}} -1 \left[\xrightarrow{\pi} +1 \xrightarrow{\pi} -1(t_1) \right]_{\kappa}, \\ 2(\wp\wp)_{AX} = 0 \xrightarrow{\frac{\pi}{2}} \mp 1 \xrightarrow{\pi} \mp 1 \xrightarrow{\frac{\pi}{2}} \pm 1 \left[\xrightarrow{\pi} \pm 1 \xrightarrow{\pi} \pm 1(t_1) \right]_{\kappa}. \end{aligned} \quad (\text{SP.4})$$

This is the set of pathways for the even-numbered echoes having an accumulated value of $\Delta p_1 = +5$ in the pulse sequence with the RF phase of the first three pulses defined in terms of ϕ_1 with every other π pulse phase set to ϕ_2 in the echo train acquisition, as shown in Fig. S2. As before, the spin transition pathways in (P.13)-(P.16) are the reflection of \wp symmetry pathways in (P.5)-(P.8) respectively about the $\wp_A = \wp_X = \wp_{AX} = 0$ without reflecting $2\wp_{AX}$ symmetry pathways. The graphical representation of transition pathways in (P.5)-(P.16) and associated symmetry pathways (SP.3)-(SP.4) is shown in Fig. S3.

Based on these desired transition pathways, the desired signals at the n^{th} echo appear at the coordinate

$$\{\Delta p_1, \Delta p_2\}_n = \{3 (-1)^{n-1}, 2 (-1)^n \lceil n/2 \rceil\} \quad \text{and} \quad \{5 (-1)^n, 2 (-1)^n \lceil n/2 \rceil\}, \quad (7)$$

where $\lceil \cdot \rceil$ is the ceiling function. The Δp_1 values for all desired odd and even echoes are fixed to $\Delta p_1 = -5, +3$ and $\Delta p_1 = +5, -3$, respectively.

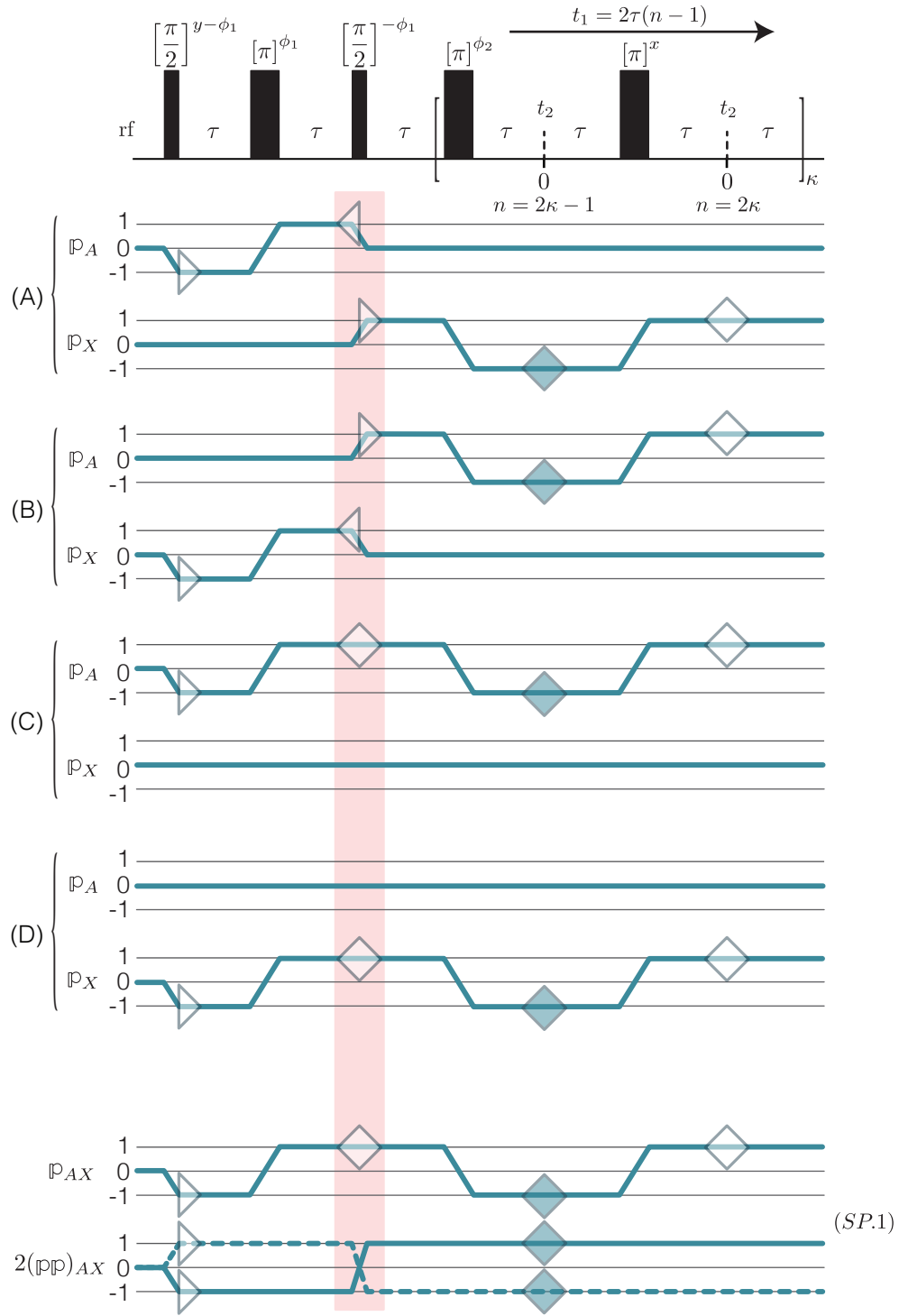


FIG. S2. A graphical representation of the symmetry pathways for the odd echoes with $\Delta p_1 = +3$. The p symmetry pathways in (A-D) are associated with spin transition pathways in (P.1–P.4) respectively. A reflection of the above p transition pathways about their respective $p_A = 0$, $p_X = 0$ and $p_{AX} = 0$ without reflecting $2d_{AX}$, gives rise to spin symmetry pathways associated with transition pathways in (P.9–P.12) respectively, for the even echoes with $\Delta p_1 = -3$.

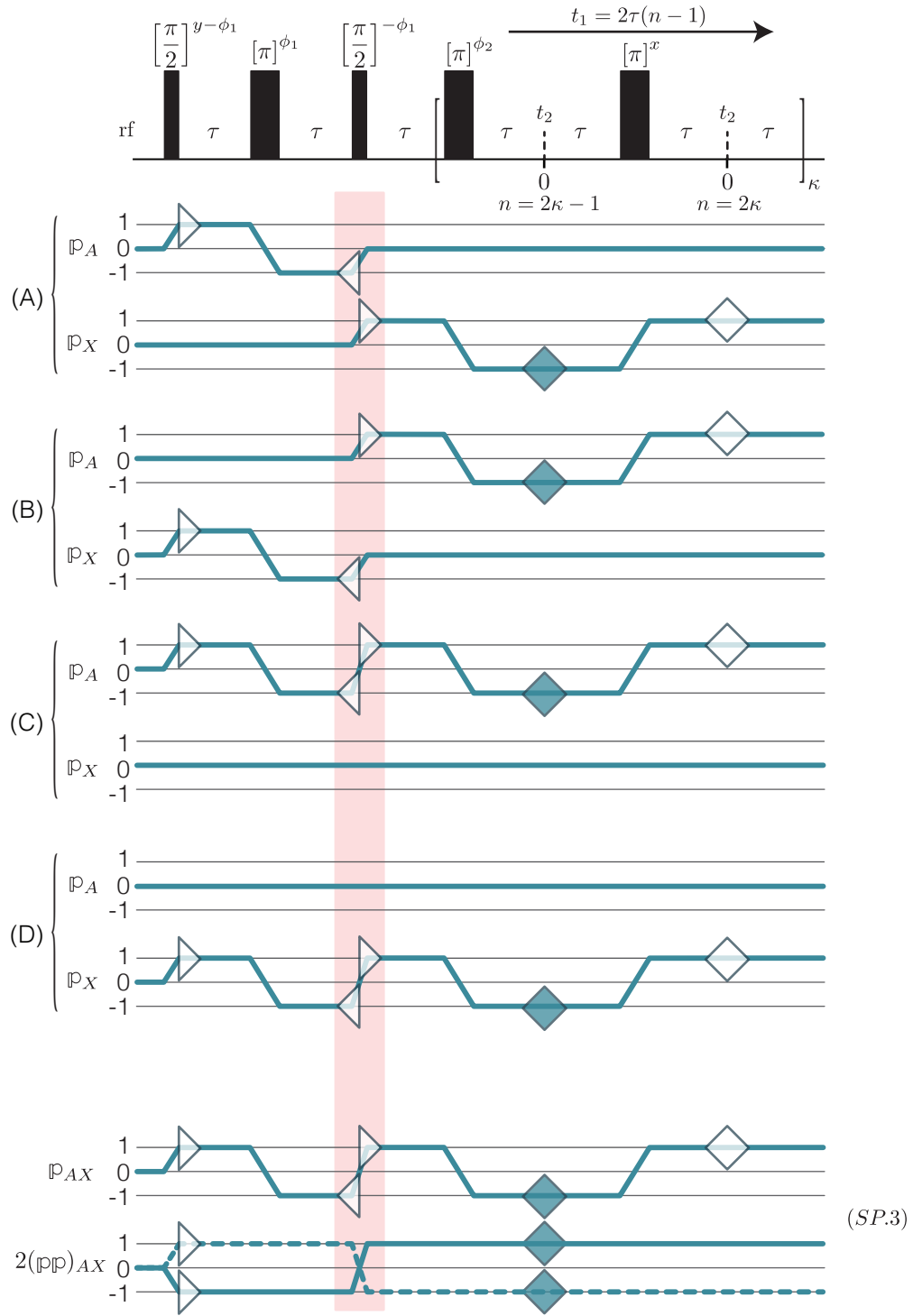


FIG. S3. A graphical representation of the symmetry pathways for the odd echoes with $\Delta p_1 = -5$. The ρ symmetry pathways in (A-D) are associated with the transition pathways in (P.5– P.8) respectively. A reflection of above ρ symmetry pathways about their respective $\rho_A = 0$, $\rho_X = 0$ and $\rho_{AX} = 0$ without reflecting $2(\rho\rho)_{AX}$, gives rise to eight symmetry pathways associated with the spin transition pathways in (P.13– P.16) respectively, for the even echoes with $\Delta p_1 = +5$.

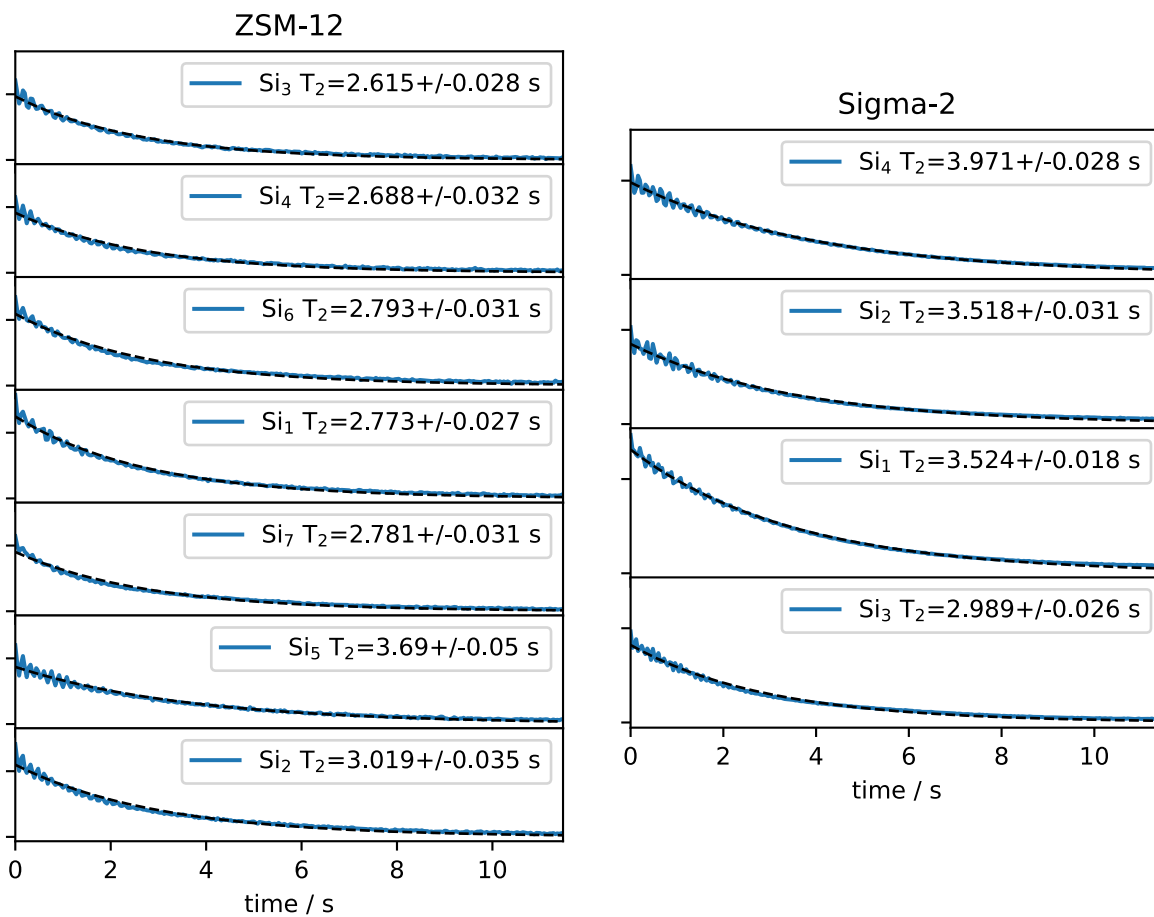


FIG. S4. Site specific ^{29}Si coherence lifetime of the rotor-synchronized π -pulse echo train during MAS in ZSM-12 and Sigma-2.

S2. RELAXATION PARAMETER FOR SIGMA-2 AND ZSM-12

The T₂ relaxation parameters for Sigma-2 and ZSM-12 are shown in Fig. S4.

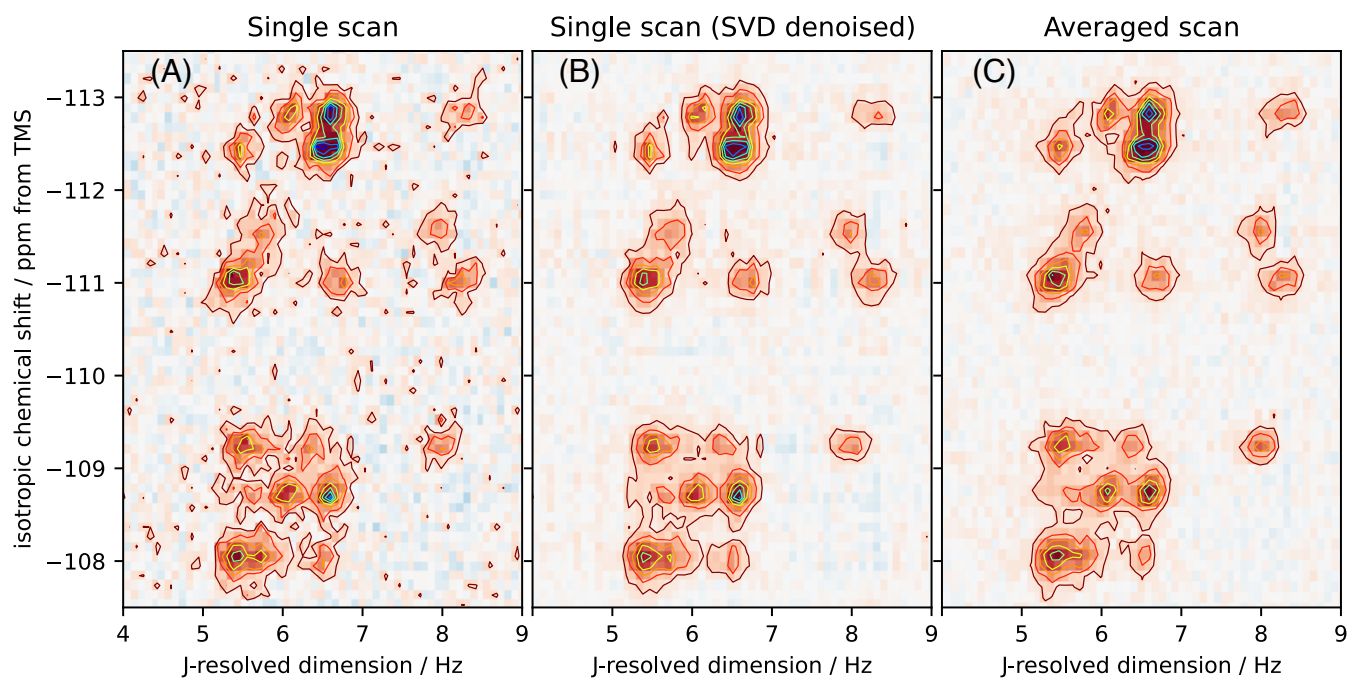


FIG. S5. Comparison of a single SE-PIETA spectra (A) with the multi-averaged SE-PIETA spectra (C) of ZSM-12. In (B) is the SVD denoised spectra of (A).

S3. SINGLE V.S. MULTI SE-PIETA AVERGED SPECTRA OF ZSM-12

The comparison of a single SE-PIETA spectra of ZSM-12 after 31.8 hours versus multi SE-PIETA averaged spectra is shown in Fig. S5.

S4. BRUKER PULSE SEQUENCES

A. SE-PIETA with t_1 interleaving

```

; p1      pi/2 pulse length
; p2      pi pulse length
; de      time to allow pulse ringdown
; l6      echo shift in rotor periods
; l29     set at runtime
; p20     saturation pulse length
; l10     number of pulses in saturation train
; pl10    power level for 90 deg and 180 deg pulses
; d20     rotor period

; cnst28  set at runtime
; cnst30  phase step interval in degree for phi2
; ns      optional 2-step phase cycle removes offset
; zgoptns : -Dsat -Dlcp15 -Dcp -Ddec -Dlacq

prosol relations=<solids_cp>

#include <Avancesolids.incl>
#include <De.incl>

; define delay tr
; "tr=1s/cnst31"          ; rotor period

"d6=d20*l6-p2/2-2*de-1u"
"d8=d6-p1/2"
"d7=(2*d20*l6-p2-4*de-aq-1u-220u)/2"
"d9=d7-0.5u"
"l7=td4/2"
"acqt0=0"
"cnst30=360/td1"          ; phase step increment in phi2
"l29=0"
"l28=0"
"l27=0"
"d12=d20*l6/td2"
"d11=l28*d12+de"
"cnst28=1.*cnst30"       ; set at runtime

#ifdef cp
; p12     power level on 1H
; p3      pulse duration corresponding to 90 degree tip angle
; pl1     power level contact during time on X channel
; sp0     power level on 1H channel
; pl2     power corresponding to 1H 90 time
; p15     contact time duration

#ifdef lcp15
#include <p15_prot.incl>
; make sure p15 does not exceed 10 msec
; let supervisor change this pulseprogram
; if more is needed
#endif
#endif

```



```

#ifdef dec
; pl12 power level during decoupling
#ifndef lacq
; disable protection file for long acquisition change
; decoupling power !!! or you risk probe damage
; if you set the label lacq (ZGOPTNS -Dlacq), the protection
; is disabled

#include <aq-prot.incl>
; allows max. 50 msec acquisition time, supervisor
; may change to max. 1s at less than 5 % duty cycle
; and reduced decoupling field
#endif
#endif

aqseq 321
1 ze
  10u st0 ; go to the first acquisition buffer
2 1u

#ifdef sat
; saturation block-----
  10u pl20:f1
20 d20
  p20:f1 ph20^
  lo to 20 times l10
; saturation block ends-----
#endif

; recycle delay-----
  d1

; calculation of phase increment/decrement-----
  "cnst28=129*cnst30" ; calculating current phi2 phase
  "cnst27=127*360/td3"
  "cnst26=360-cnst27"
  "d11=-128*d12+-de"

; First, pulse with positive phase phi1 -----
  1u ip1 + cnst26
#ifdef cp
  1u fq=cnst21:f2
  10u pl1:f1
  (p3 pl2 ph6):f2
  (p15 pl1 ph1):f1 (p15:sp0 ph10):f2
#else
  10u pl10:f1
  (0.5u pl10 ph1):f1
  (p1):f1
#endif

#ifdef dec
  de cpds2:f2
#else
  de
#endif
  d6 pl10:f1
  de ip2+cnst27

```

```

; Second, 180 pulse with negative phase phi1 -----
#ifdef dec
    0.5u ;do:f2
#else
    0.5u
#endif
    (0.5u pl10 ph2):f1
    (p2):f1
#ifdef dec
    de ;cpds2:f2
#else
    de
#endif
    d8
    de ip3+cnst26

; Third, 90 pulse with positive phase phi1 -----
#ifdef dec
    0.5u ;do:f2
#else
    0.5u
#endif
    (0.5u pl10 ph3):f1
    (p1):f1
#ifdef dec
    de ;cpds2:f2
#else
    de
#endif
    d8 ip4+cnst28          ; presetting current negative phi2
    d11

; Fourth, 180 pulse with negative phase phi2 -----
3 0.1u
#ifdef dec
    0.4u ;do:f2
#else
    0.4u
#endif
    (0.5u pl10 ph4):f1
    (p2):f1
#ifdef dec
    0.5u ;cpds2:f2
#else
    0.5u
#endif
    d7
    d11
    110u

; Acquisition Block -----
ACQ_START(ph30,ph29) ; macro with acquisition prep delays - contains de
aq DWELLGEN:f1
100u eoscp          ; eoscp should be at least 100 us, end of scan

```

```

    10u st          ; advance to next acq buffer
    d7
    de              ; st requires 10 us, so two de delays should always be enough
#ifdef dec
    de ;do: f2
#else
    de
#endif

; Fifth, 180 pulse without any phase -----
    (0.5u pl10 ph5):f1
    (p2):f1
#ifdef dec
    de ;cpds2: f2
#else
    de
#endif
    d7
    0.5u
    110u

; Acquisition Block-----
    ACQ_START(ph30,ph31) ;macro containing delays to prep for acquisition — contains de
    aq DWELLGEN: f1
    100u eoscp          ; eoscp should be at least 100 us, end of scan
    10u st              ; advance to next acq buffer
    de
    d9
    de

    "d11=-de"
    lo to 3 times l7
#ifdef dec
    0.5u do: f2
#else
    0.5u
#endif
#ifdef dec
    lo to 2 times ns
    30m wr #0 if #0 zd
    "l27=l27+1"
    lo to 2 times td3
    "l27=0"
    "l28=l28+1"
    lo to 2 times td2
    "l28=-0"
    "l29=l29+1"
    lo to 2 times td1

HaltAcqu, lm
exit

#ifdef cp
ph1 = 0
ph6 = 1
#else
ph1 = 1
#endif

```

```
ph2 = 0  
ph3 = 0
```

```
ph4 = 0  
ph5 = 0  
ph10 = 0  
#ifdef sat  
    ph20= 0  
#endif
```

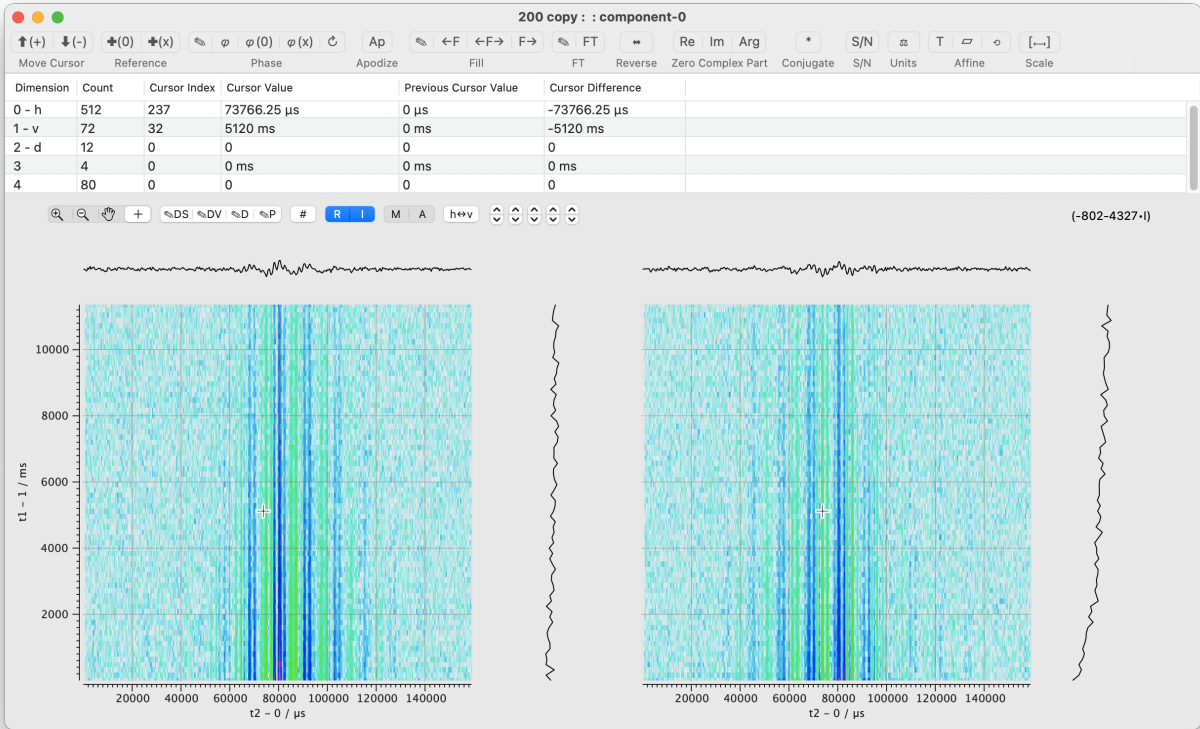
```
ph30= 0  
ph29= 0  
ph31= 0
```

S5. INTERLEAVED SHIFTED-ECHO PIETA SIGNAL PROCESSING

We implement the interleaved shifted-echo PIETA sequence for this work using two phase dimensions. In this section, we provide a step-by-step guide with a graphical illustration for the processing of 5D interleaved SE-PIETA signal, $s(\phi_2, \tau_1, \phi_1, n, t_2)$, where t_2 is the time dimension, n is the echo count dimension, τ_1 is the interleave delay dimension, and ϕ_1 and ϕ_2 are the two phase dimensions. The Fourier transform with respect to the ϕ_2 phase dimension gives the Δp_1 dimension—the accumulated change in coherence order through the first three pulses of the preparation period—and is used to obtain the desired pathways in the preparation period of Figs. S2 and S3. Here, we implement a 12 step ϕ_1 phase dimension. The Fourier transform with respect to the ϕ_2 phase dimension gives the Δp_2 dimension—the accumulated change in coherence order through the subsequent π pulses leading up to the n^{th} echo—and is used to obtain the desired echo train pathways in Figs. S2 and S3. A step-by-step guide to the spectral processing using *RMN*[5] is given below.

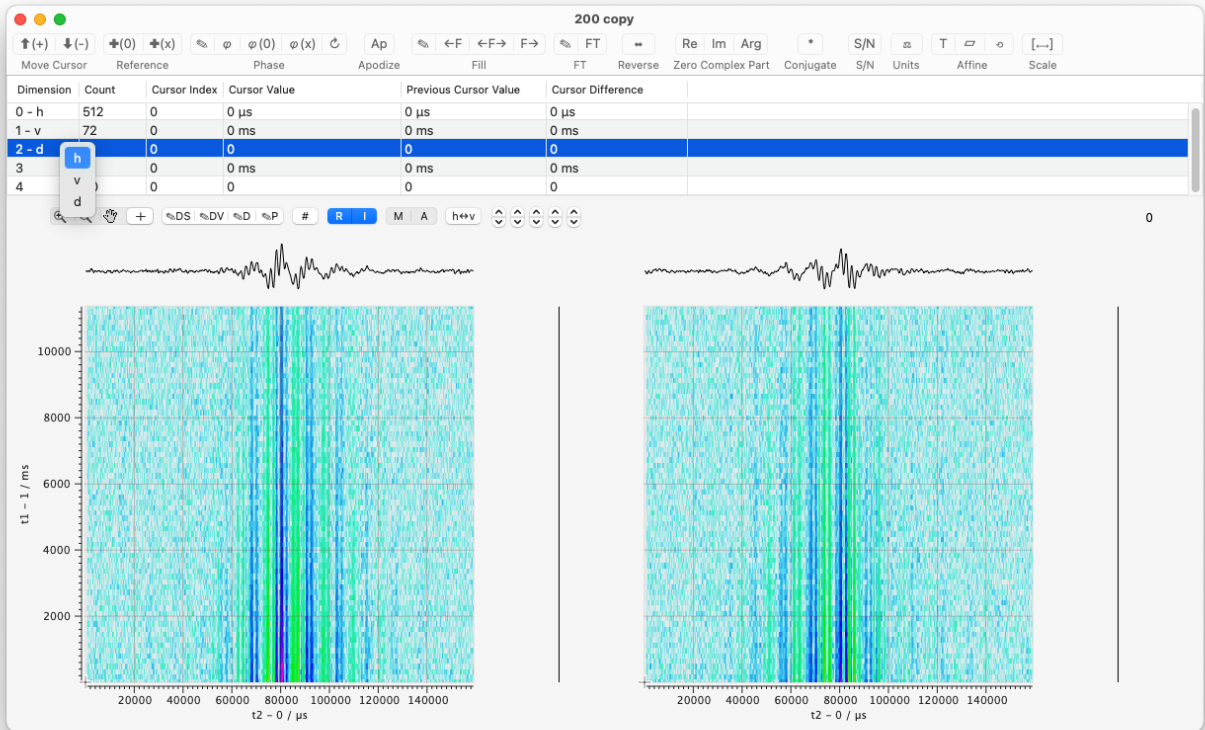
Below is the RMN window displayed after opening the file 200.csd, available in the supplemental material on Zenodo, which contains the ^{29}Si interleaved shifted-echo PIETA signal for sigma-2. Additional details about the RMN user interface can be found by hovering the cursor over each icon and menu command. The RMN window below shows color intensity plots of the real and imaginary parts of 2D cross-sections of the 5D signal. You change to the cursor position inside the displayed 2D cross-section with the mouse or using the arrow keys on the keyboard. Additionally, the cursor index, and the displayed 2D cross-section, can be changed by clicking on the up or down arrows in the icon $\updownarrow\updownarrow\updownarrow\updownarrow$. In the example window below, each arrow pair corresponds to one of the five dimensions. One-dimensional cross-sections along the horizontal and vertical dimensions taken at the cursor position, i.e., the focus of the dataset, are also displayed above and to the right of the 2D intensity plot.

Above the cross-section color intensity plots is an interactive table with information on each of the five dimensions in this dataset. Here, the rows with dimension indexes 0 to 4 are associated with the dimensions for t_2 , t_1 , ϕ_1 , τ_1 , and ϕ_2 , respectively.

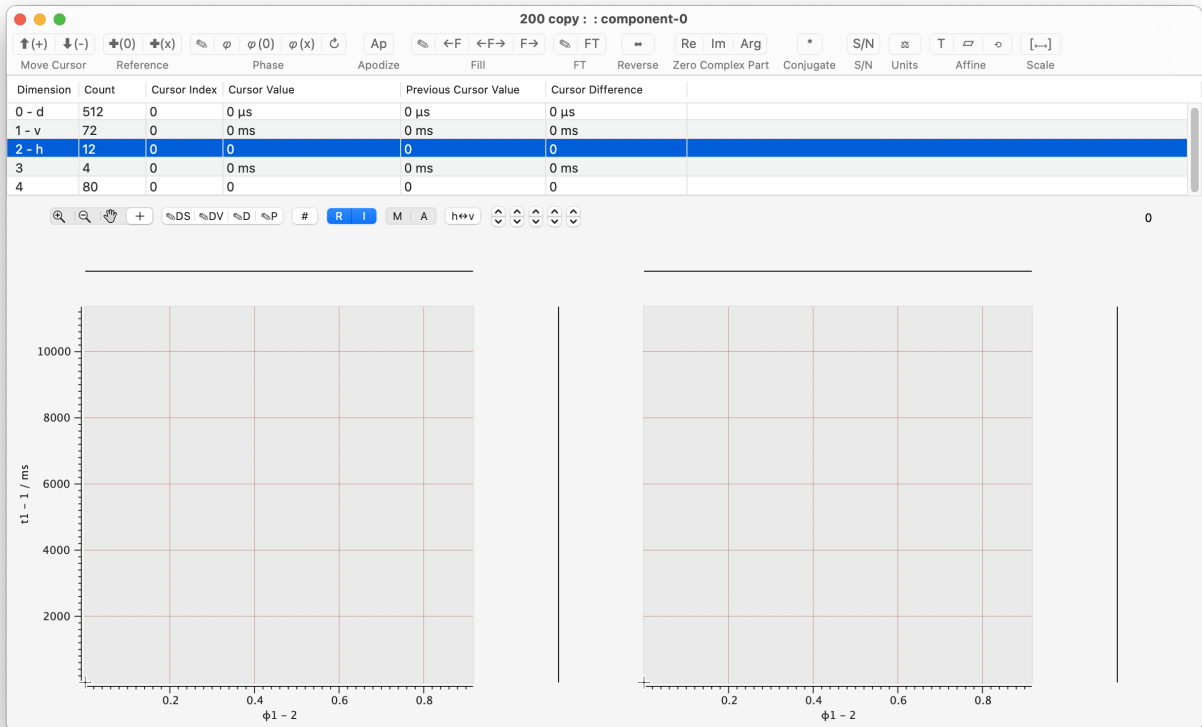


In RMN, all signal processing is performed according to the defined dimension precedence. That is, 1D signal processing is performed along the horizontal dimension, 2D signal processing is performed along the horizontal and vertical dimensions, and 3D signal processing is performed along the horizontal, vertical, and depth dimensions. In this guide, we only need to assign the horizontal and/or vertical dimensions before performing processing functions.

1. The first step in processing the sigma-2 dataset is to assign the ϕ_1 (index 4) dimension to the horizontal dimension. This is done by selecting the row for the dimension in the table, right-clicking on the dimension column, and selecting the precedence assignment (h,v, or d) from the pop-up window, as shown below.

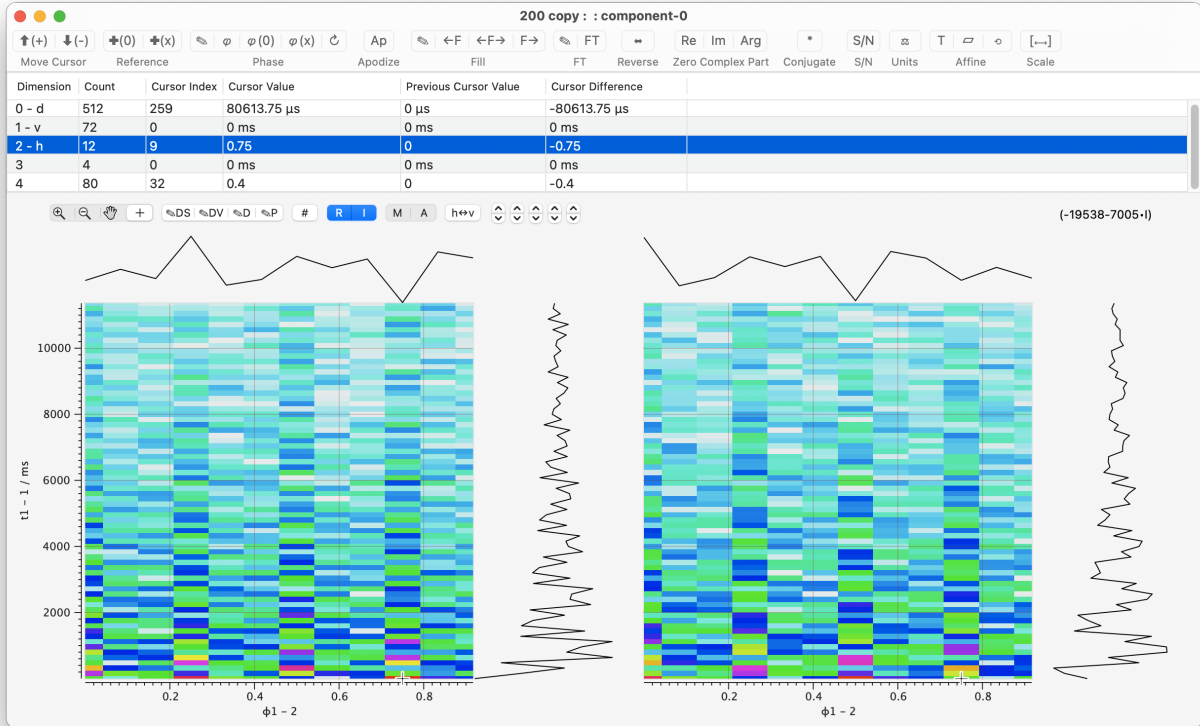


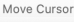
After assigning the ϕ_1 (index 4) dimension to the horizontal dimensions, the window will appear as shown below.

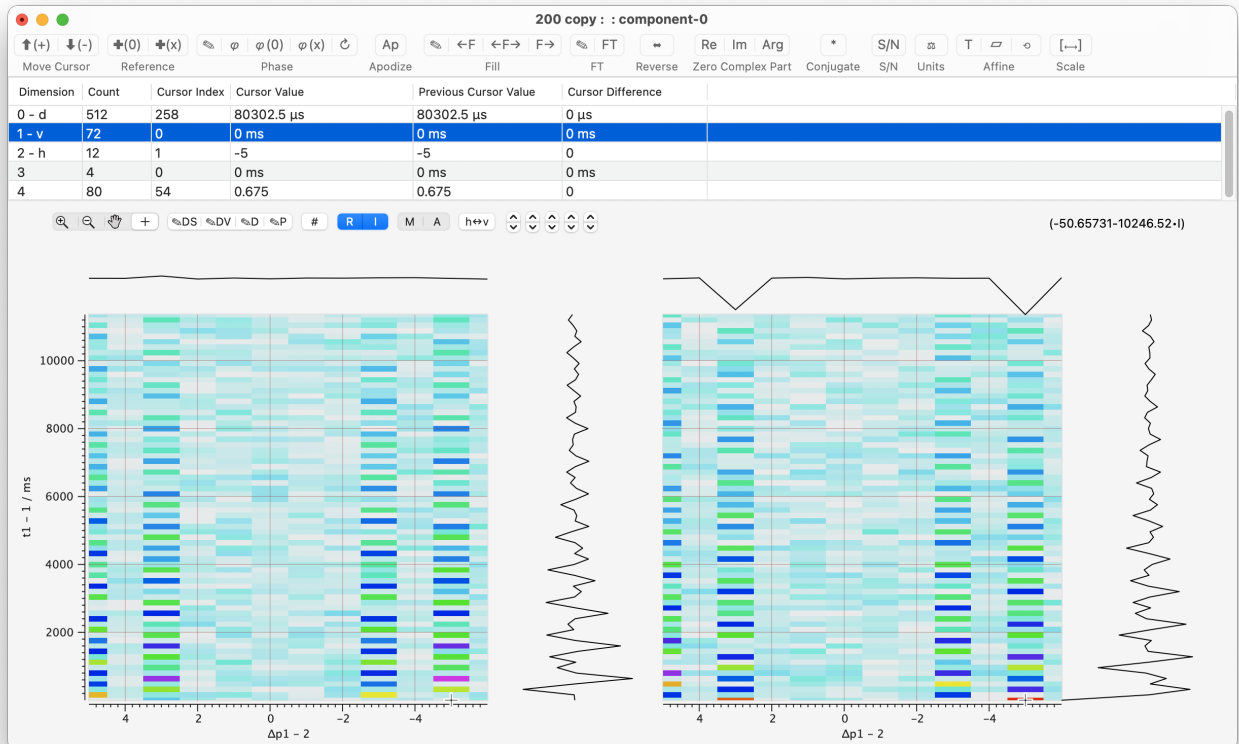


While there is little to no signal in the displayed cross-section, you can move the cursor, i.e., the focus, to the dependent variable maximum by clicking on the up arrow button in $\uparrow(+)$ $\downarrow(-)$ as shown below.

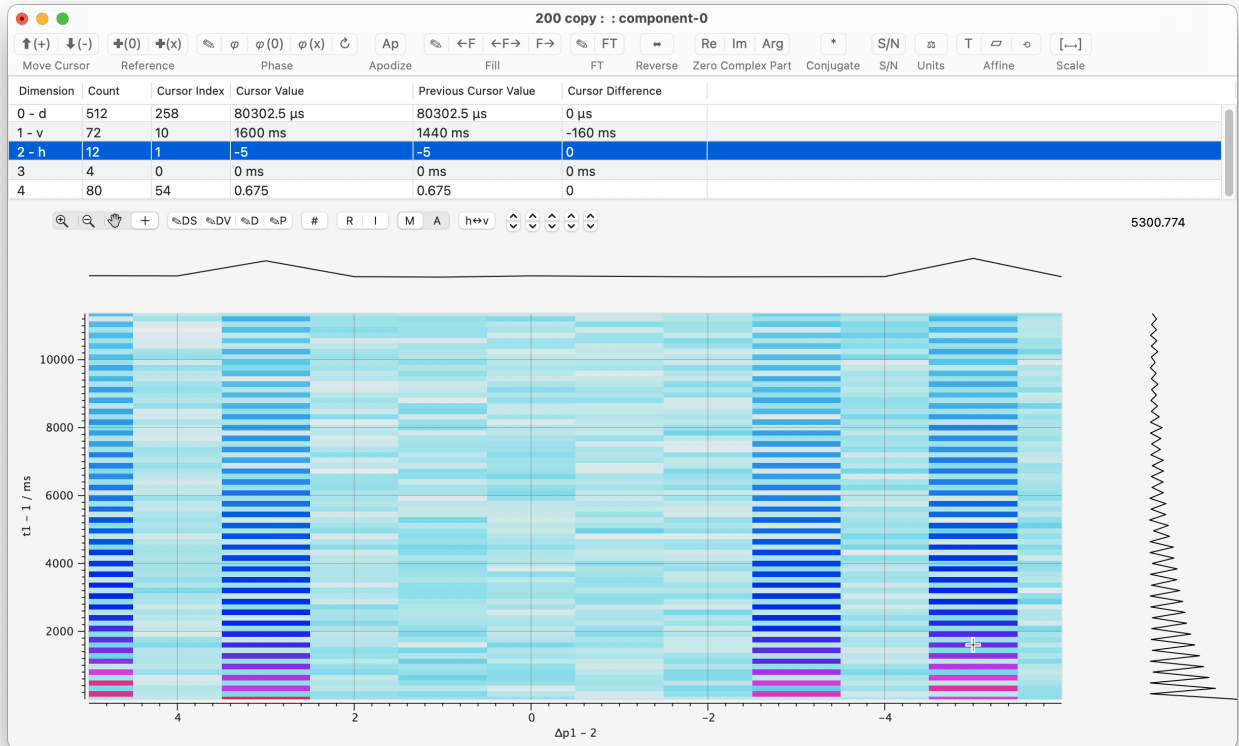
Move Cursor



2. Next, we perform a Fourier transform along the ϕ_1 dimension to transform the 5D signal $s(\phi_2, \tau_1, \phi_1, t_1, t_2)$ to $s(\phi_2, \tau_1, \Delta p_1, t_1, t_2)$ where Δp_1 is the accumulated change in coherence order through the first three pulses. Command-F performs a Fourier transform along the horizontal dimension, i.e., the ϕ_2 dimension. Clicking on the up arrow button in , moves to the cross-section of maximum intensity as shown below.



To view the magnitude mode signal, click the M button in the **R I M A** control just below the table.

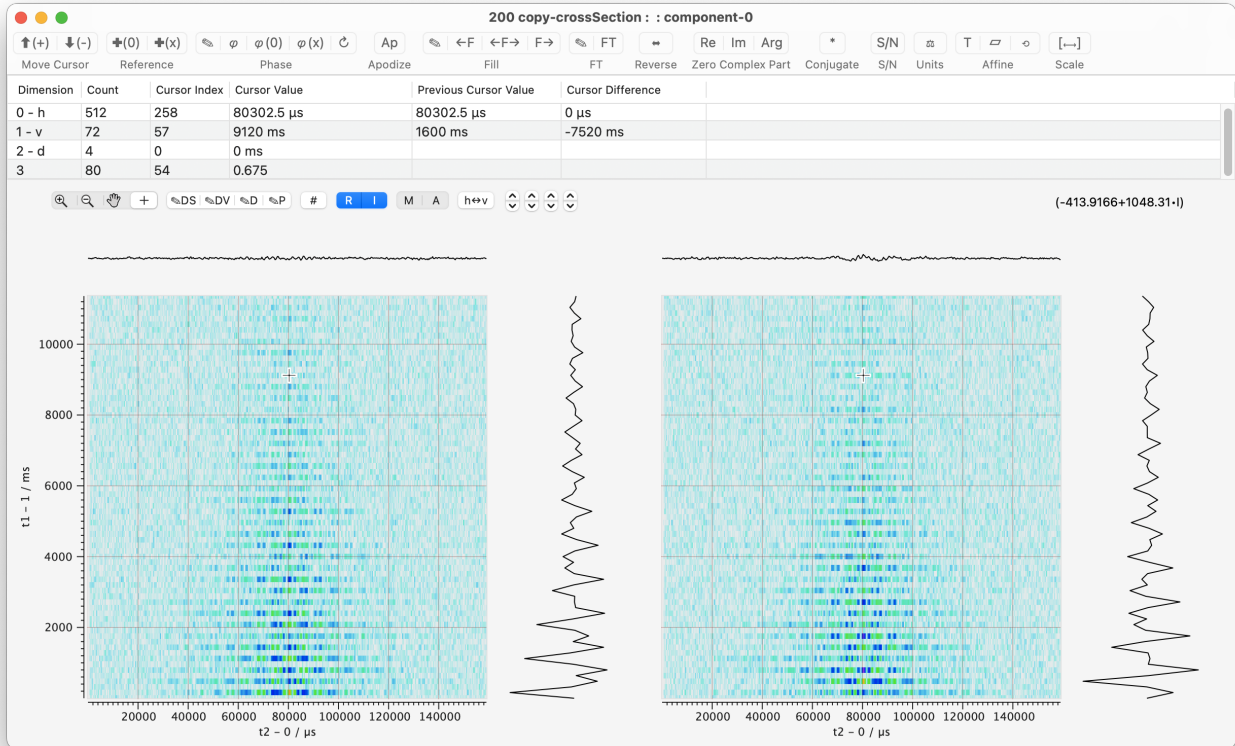


Notice that the odd echoes have maximum intensity at $\Delta p_1 = -5$ and $\Delta p_1 = +3$ while the even echoes have maximum intensity at $\Delta p_1 = +5$ and $\Delta p_1 = -3$.

To switch back to the view of the real and imaginary parts of the signal, click on the R and I buttons in the **R I M A** control right below the table.

From this 5D signal, we will extract four 4D signals, by selecting the 4D cross-sections at $\Delta p_1 = -5$, $\Delta p_1 = +3$, $\Delta p_1 = -3$, and $\Delta p_1 = +5$. The following steps illustrate only the extraction and processing of the $\Delta p_1 = +5$ cross-section. Do not close the original RMN window (shown above), as it will be needed to extract all four Δp_1 cross-sections.

- Position the cursor on the $\Delta p_1 = +5$ cross-section, using either the mouse or keyboard arrow keys to get +5 under cursor value in the table for the row labeled 2-h. With the cursor in place, go to the **Create** menu, and select the **by extracting cross-section along vertical dimension at cursor** menu item. Alternatively, right-clicking on the vertical 1D cross-section shown to the right of the 2D intensity plot will perform the same function. This will create the 4D cross-section signal, $s_{+5}(\phi_2, \tau_1, t_1, t_2)$, as shown below.



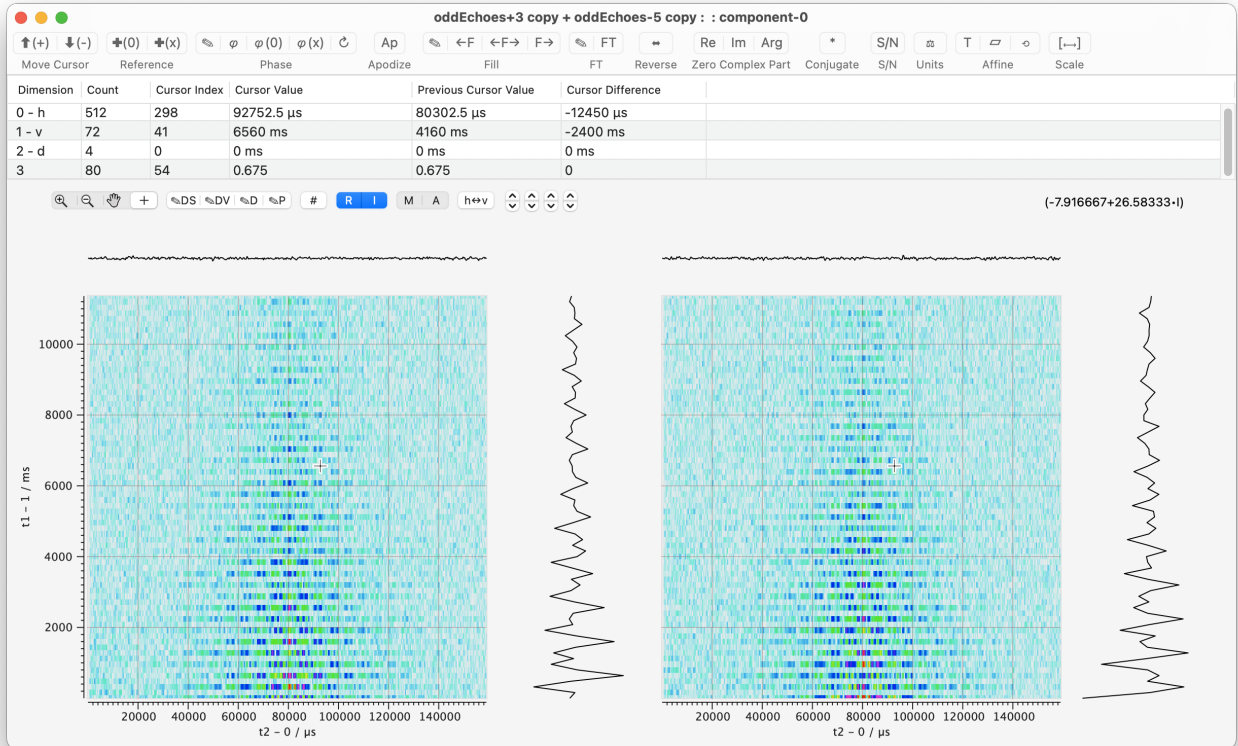
4. Save this 4D dataset as “evenEchoes+5.π” and close this window.
5. Go back to the original 5D dataset, and position the cursor on the $\Delta p_1 = +3$ cross section, extract the cross-section, and save this 4D dataset as “oddEchoes+3.π”. This will create the 4D cross-section signal, $s_{+3}(\phi_2, \tau_1, t_1, t_2)$. Close this window.
6. Again, go back to the original 5D dataset, and position the cursor on the $\Delta p_1 = -3$ cross section, extract the cross-section, and save this 4D dataset as “evenEchoes-3.π”. This will create the 4D cross-section signal, $s_{-3}(\phi_2, \tau_1, t_1, t_2)$. Close this window.
7. Once last time, go back to the original 5D dataset, and position the cursor on the $\Delta p_1 = -5$ cross section, extract the cross-section, and save this 4D cross-section as “oddEchoes-5.π”. This will create the 4D cross-section signal, $s_{-5}(\phi_2, \tau_1, t_1, t_2)$. Close this window.
8. You can now close the original (and remaining) RMN window.




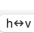
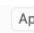
-
9. Next, we create the odd echoes dataset

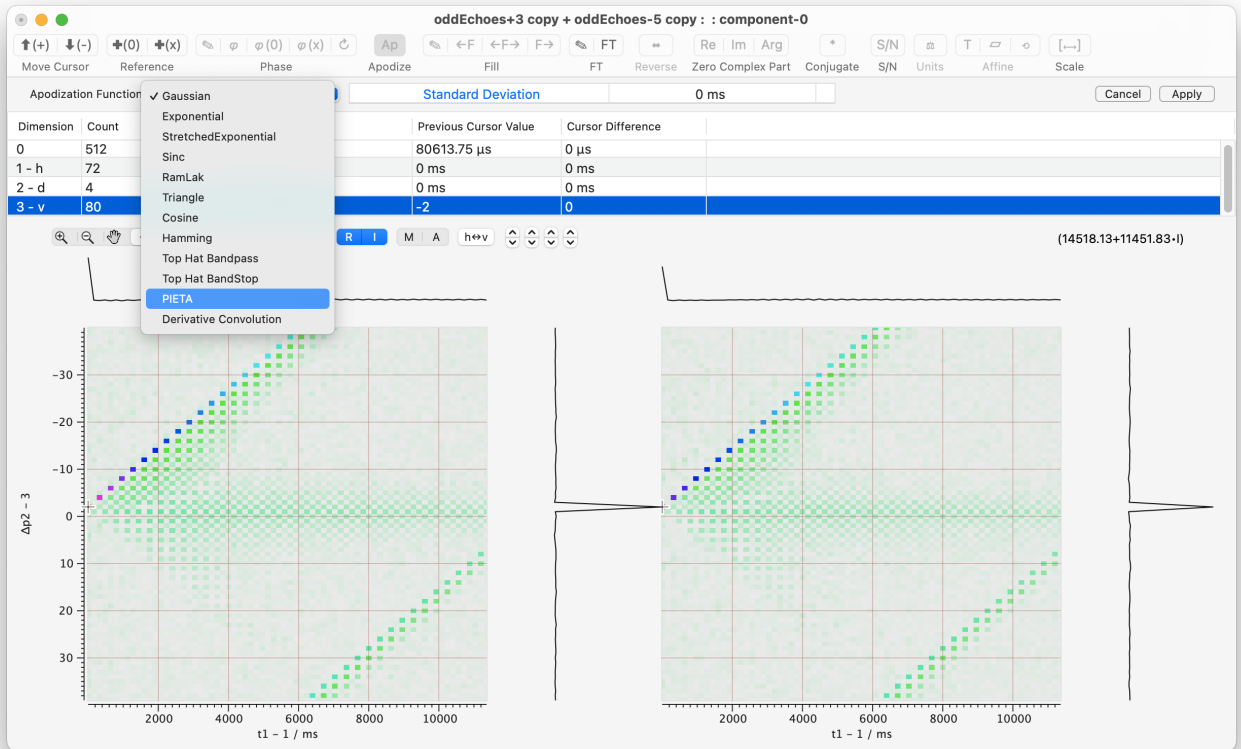
$$s_{\text{odd}}(\phi_2, \tau_1, t_1, t_2) = s_{+3}(\phi_2, \tau_1, t_1, t_2) + s_{-5}(\phi_2, \tau_1, t_1, t_2). \quad (8)$$

Use RMN to open the dataset file “oddEchoes+3.π”.

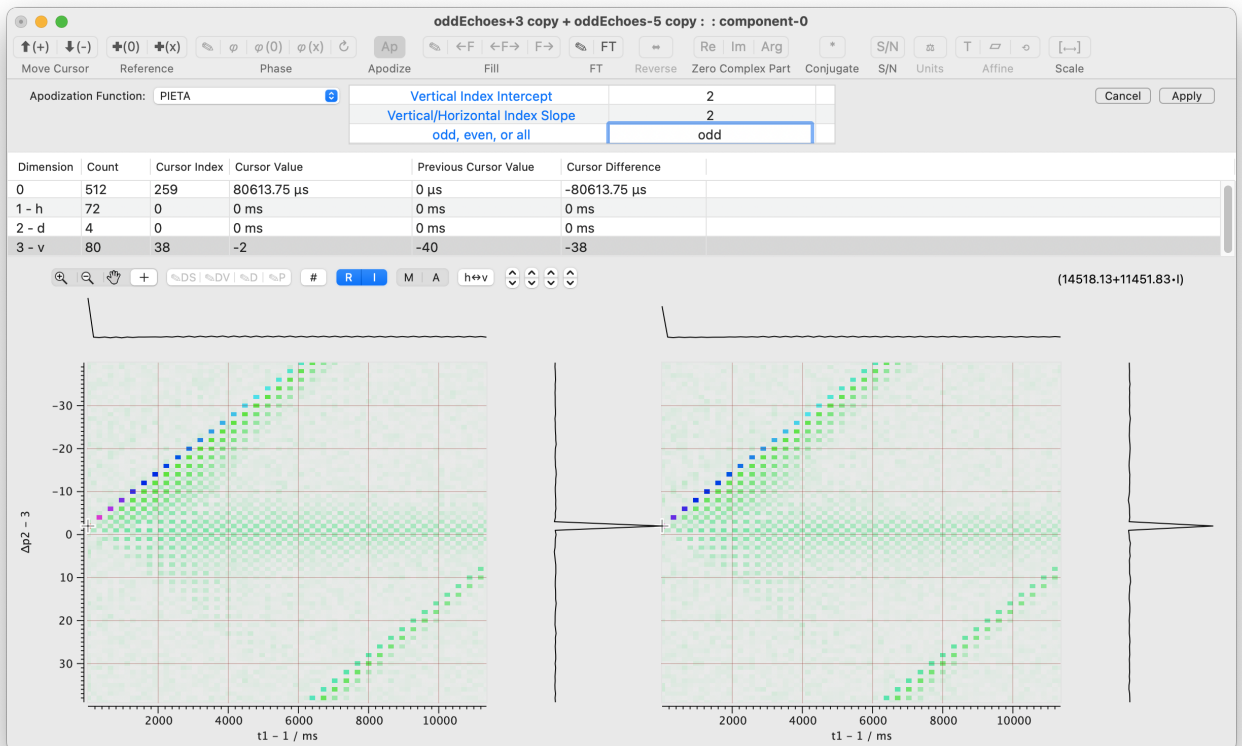
10. Once the dataset is open, under the **Create** menu select the menu item **By adding in another dataset...**. This command brings up an open file dialog. Select the file “oddEchoes-5.π”. This will create a new RMN window with the 4D dataset $s_{\text{odd}}(\phi_2, \tau_1, t_1, t_2)$.



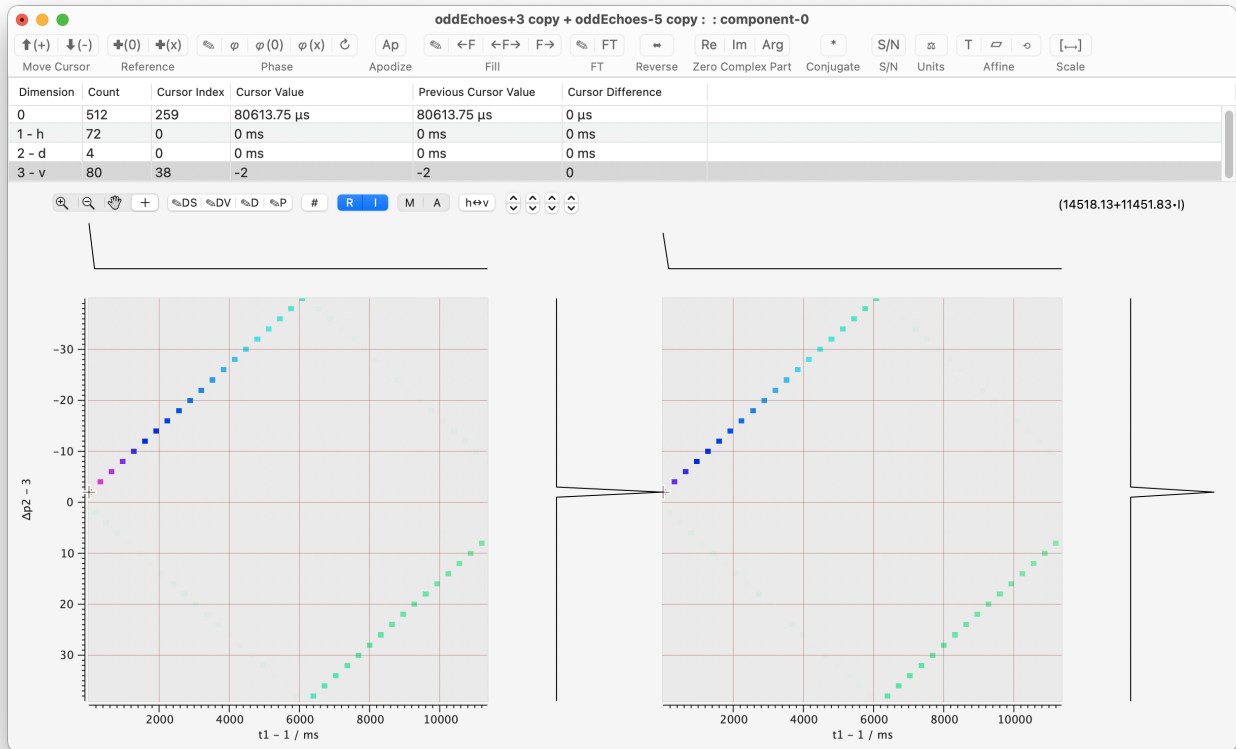
- Place the ϕ_1 (index 3) dimension along the horizontal dimension. Move the cursor to the dependent variable maximum, i.e., the up arrow button in , and click on the unzoom button, i.e., the magnifying glass with the “-” inside, i.e., the 2nd button in .
- Apply a FT (command-F) to convert the 4D cross-section signal from $s_{\text{odd}}(\phi_2, \tau_1, t_1, t_2)$ to $s_{\text{odd}}(\Delta p_2, \tau_1, t_1, t_2)$, and move the cursor to the dependent variable maximum, i.e., the up arrow button in .
- Click on the  button to swap the horizontal-vertical dimension precedence.
- Click on the  button to bring up the Apodization dialog panel at the top of the window, and select the PIETA apodization from the pop-up menu as shown below.



15. Enter 2 for the Vertical Index Intercept, 2 for the Vertical/Horizontal Index Slope, and "odd" for the odd, even or All parameter.



16. Applying this apodization eliminates undesired symmetry pathway signals during the echo train acquisition.

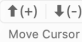

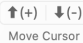




17. Save this dataset as “oddEchoes. π ”. Close all RMN Windows.

18. Next, we create the even echoes dataset

$$s_{\text{even}}(\phi_2, \tau_1, t_1, t_2) = s_{+5}(\phi_2, \tau_1, t_1, t_2) + s_{-3}(\phi_2, \tau_1, t_1, t_2). \quad (9)$$

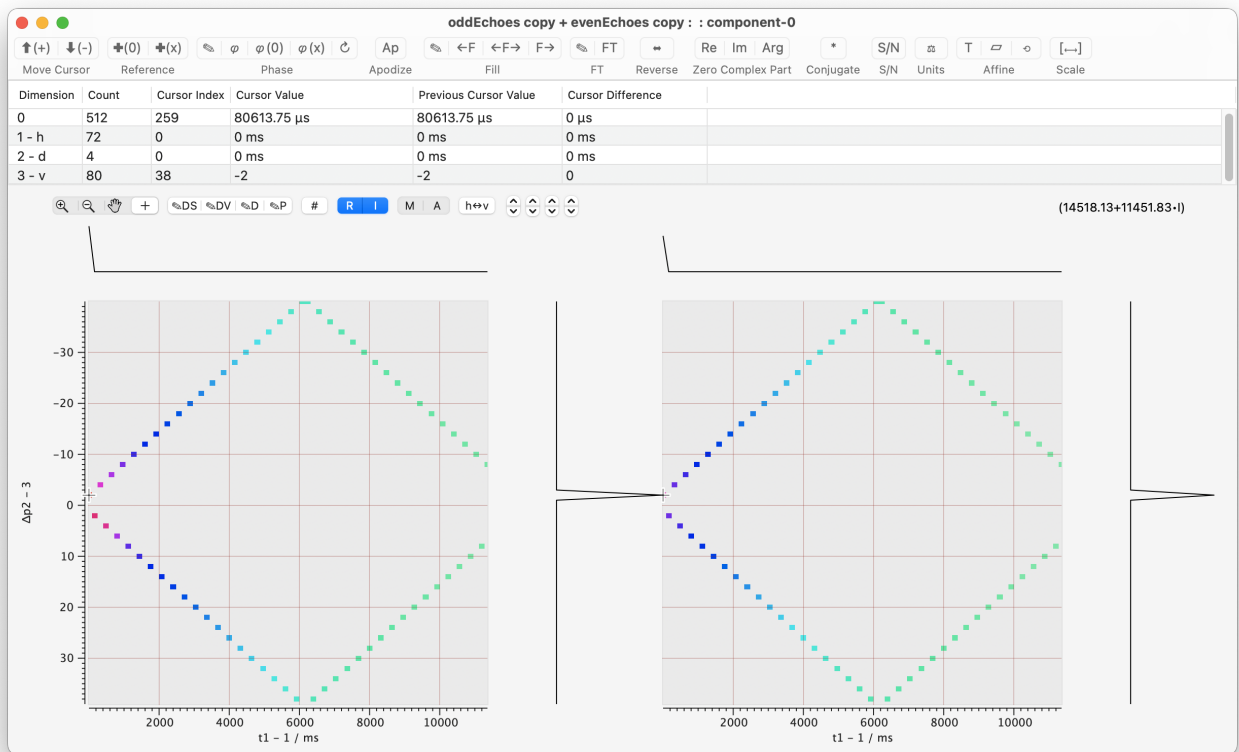
Use RMN to open the dataset file “evenEchoes+5. π ”.

19. Once the dataset is open, from the menu **Create** go to the submenu **By adding in another dataset...**. This command brings up an open file dialog. Select the file “evenEchoes-3. π ”. This will create a new RMN window with the 4D dataset $s_{\text{even}}(\phi_2, \tau_1, t_1, t_2)$.
20. Place the ϕ_1 (index 3) dimension along the horizontal dimension. Move the cursor to the dependent variable maximum, i.e., the up arrow in , and click on the unzoom icon—the magnifying glass with the “-” inside, i.e., the 2nd button in .
21. Apply a FT (command-F) to convert the 4D cross-section signal from $s_{\text{even}}(\phi_2, \tau_1, t_1, t_2)$ to $s_{\text{even}}(\Delta p_2, \tau_1, t_1, t_2)$, and move the cursor to the dependent variable maximum, i.e., the up arrow in .
22. Click on the  button to swap the horizontal-vertical dimension precedence.
23. Click on the  button to bring up the Apodization dialog panel in the top section of the window, and select the PIETA apodization from the pop-up menu.
24. Enter 2 for the Vertical Index Intercept, 2 for the Vertical/Horizontal Index Slope, and “even” for the odd, even or All parameter to eliminate the undesired symmetry pathway signals during the echo train acquisition.
25. Save this dataset as “evenEchoes. π ”. Close all RMN Windows.

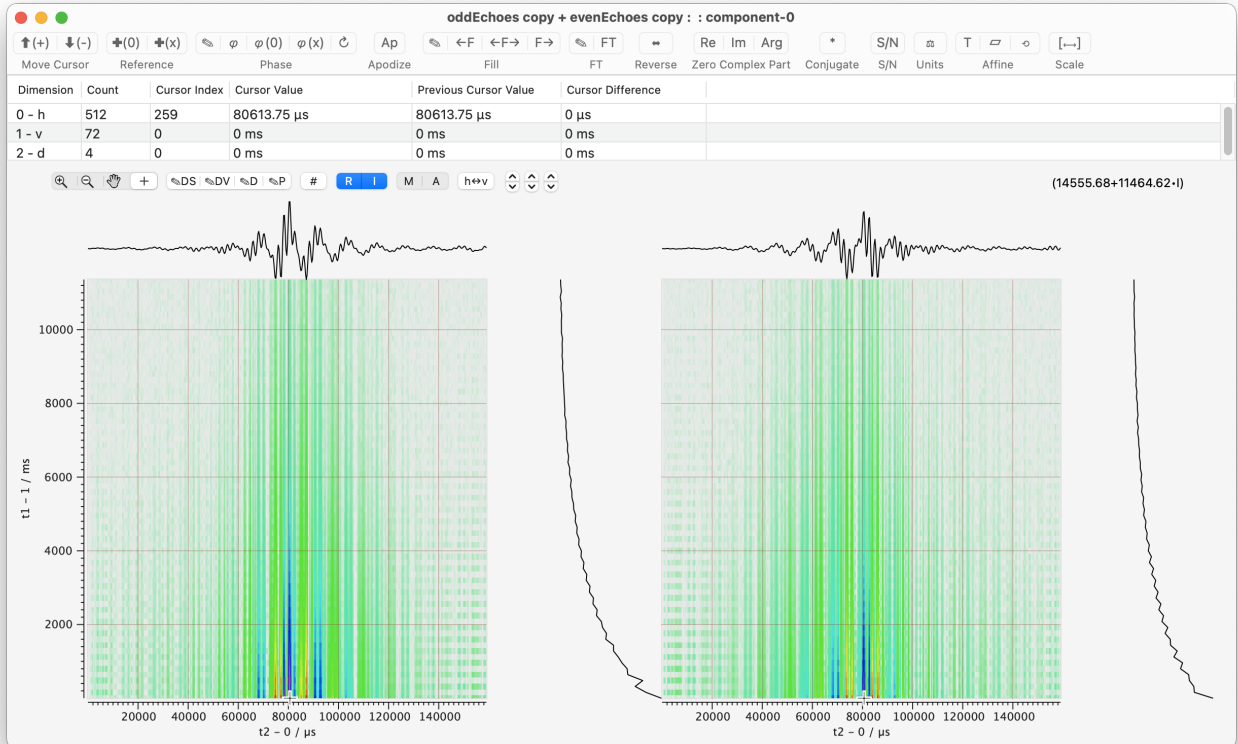
26. Reopen the “oddEchoes. π ” dataset. Under the **Create** menu, select the **By adding in another dataset...** menu item. This command brings up a open file dialog. Select the file “evenEchoes. π ”. This will create the 4D signal $s(\Delta p_2, \tau_1, t_1, t_2)$, i.e.,

$$s(\Delta p_2, \tau_1, t_1, t_2) = s_{\text{odd}}(\Delta p_2, \tau_1, t_1, t_2) + s_{\text{even}}(\Delta p_2, \tau_1, t_1, t_2), \quad (10)$$

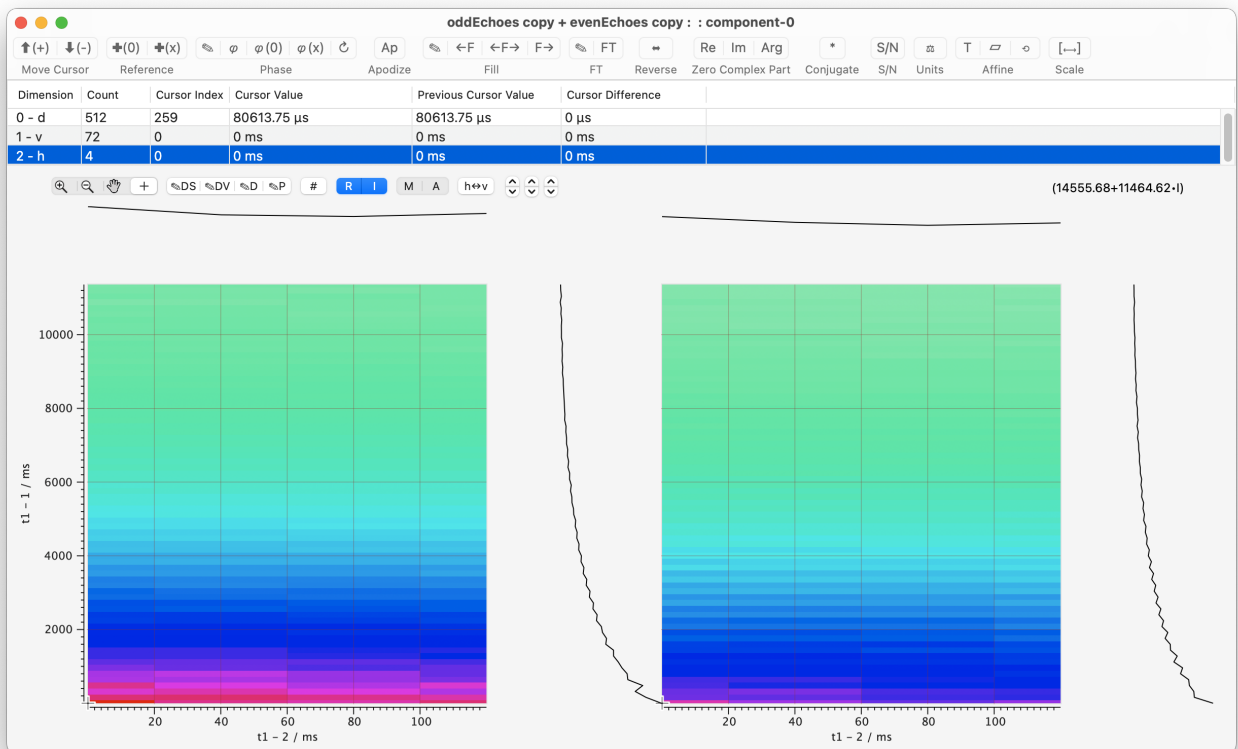
shown below.



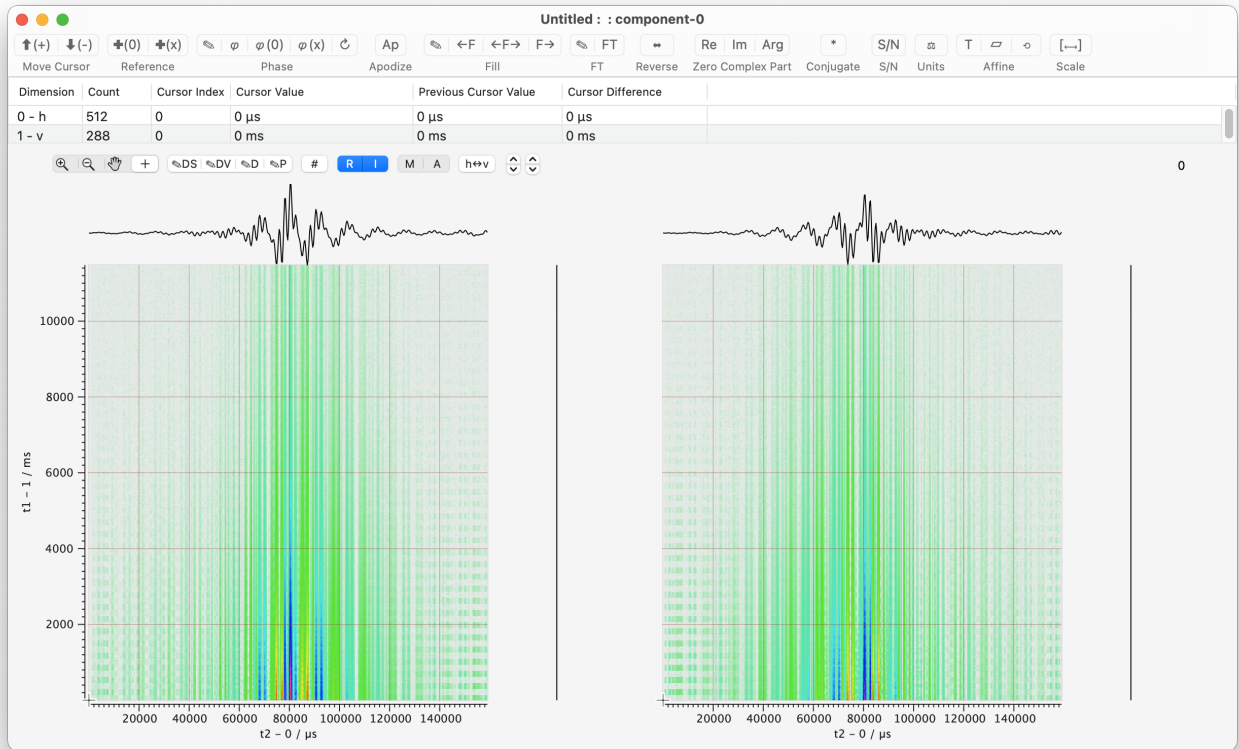
27. Under the menu **Create** and the **By projecting out dimension** submenu, select the **Project out vertical: full**. This integrates over the Δp_2 dimension, creating the 3D cross-section signal $s(\tau_1, t_1, t_2)$ shown below.



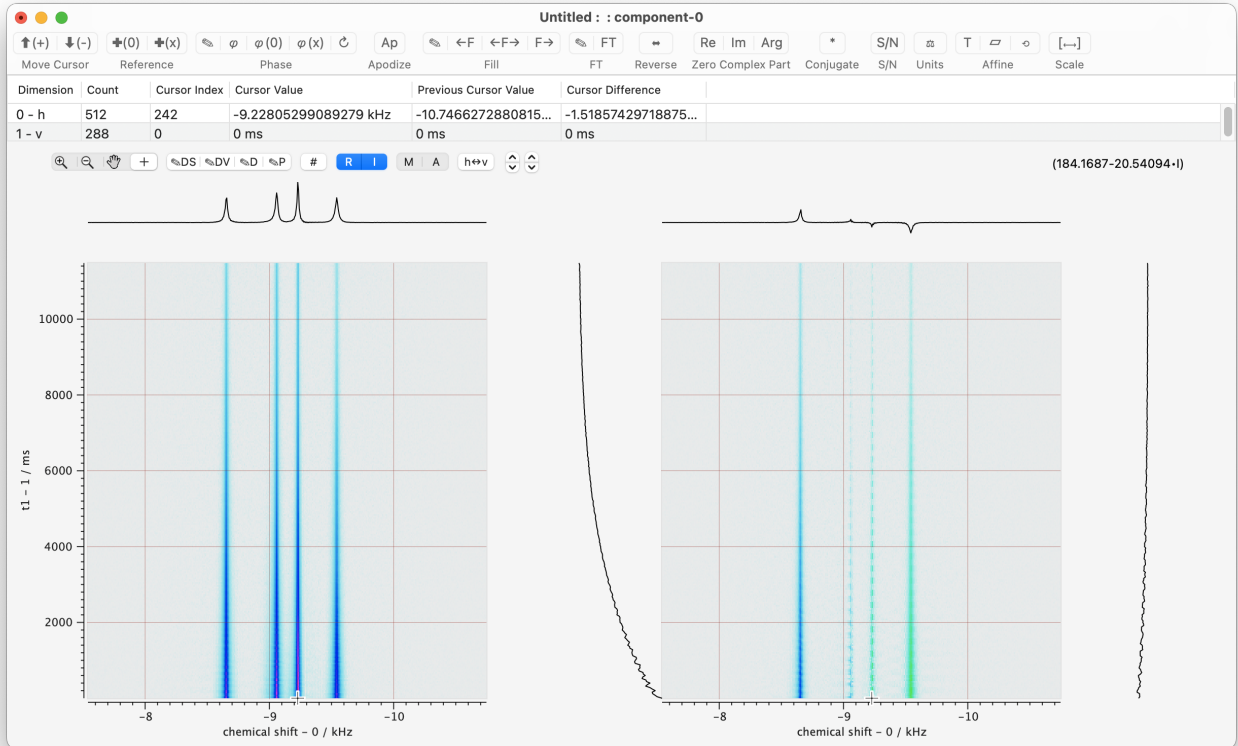
28. Using the dataset $s(\tau_1, t_1, t_2)$ in the current window, place the τ_1 (index 2) dimension along the horizontal and the t_1 (index 1) dimension along the vertical.



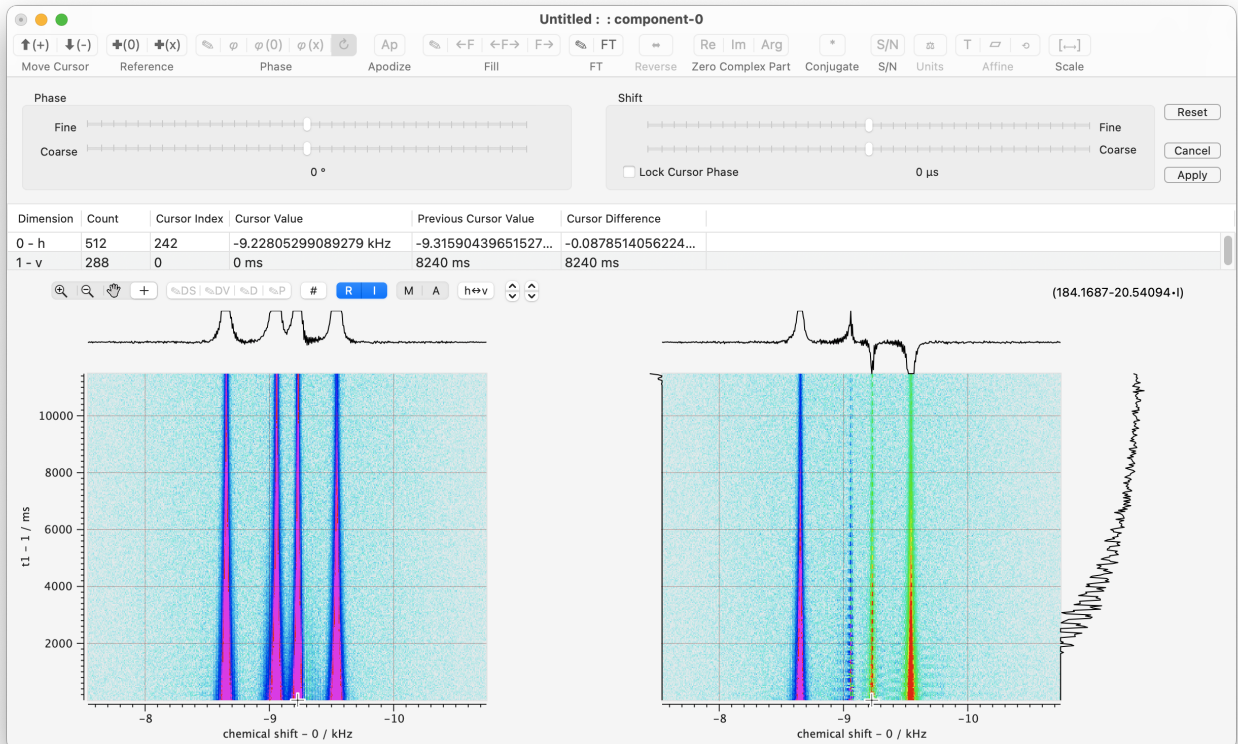
29. Under the **Create** menu, select the **By appending responses along vertical onto horizontal dimension** menu item. This will create the 2D signal, $s(t_1, t_2)$, in a new window as shown below.



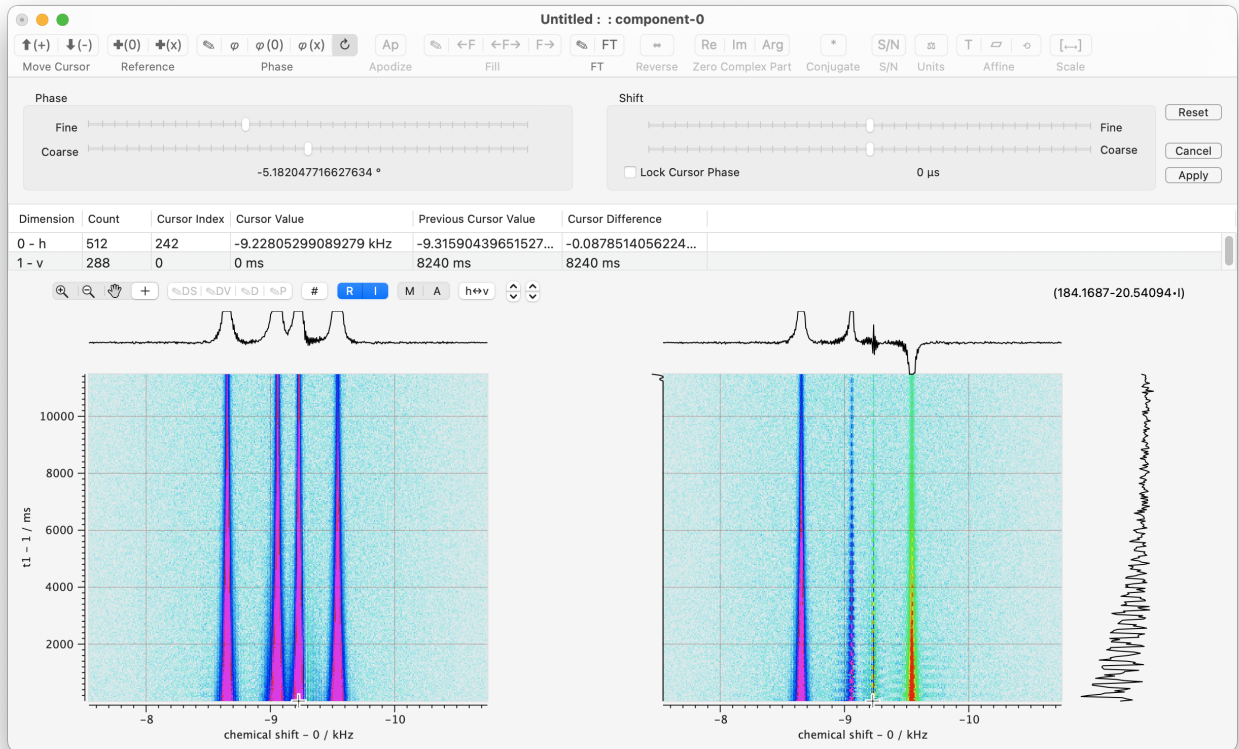
30. In the window above, move the Cursor to the dependent variable maximum, i.e., click on the up arrow button in $\uparrow(+)$ $\downarrow(-)$. Set the cursor coordinates to zero, i.e., click on the $+(0)$ button in $\uparrow(+)$ $\downarrow(-)$. Phase the origin, i.e., click on the $\phi(0)$ button in ϕ $\phi(0)$ $\phi(x)$ ϕ . Apply a FT (command-F) to transform $s(t_1, t_2)$ into $s(t_1, \omega_2)$



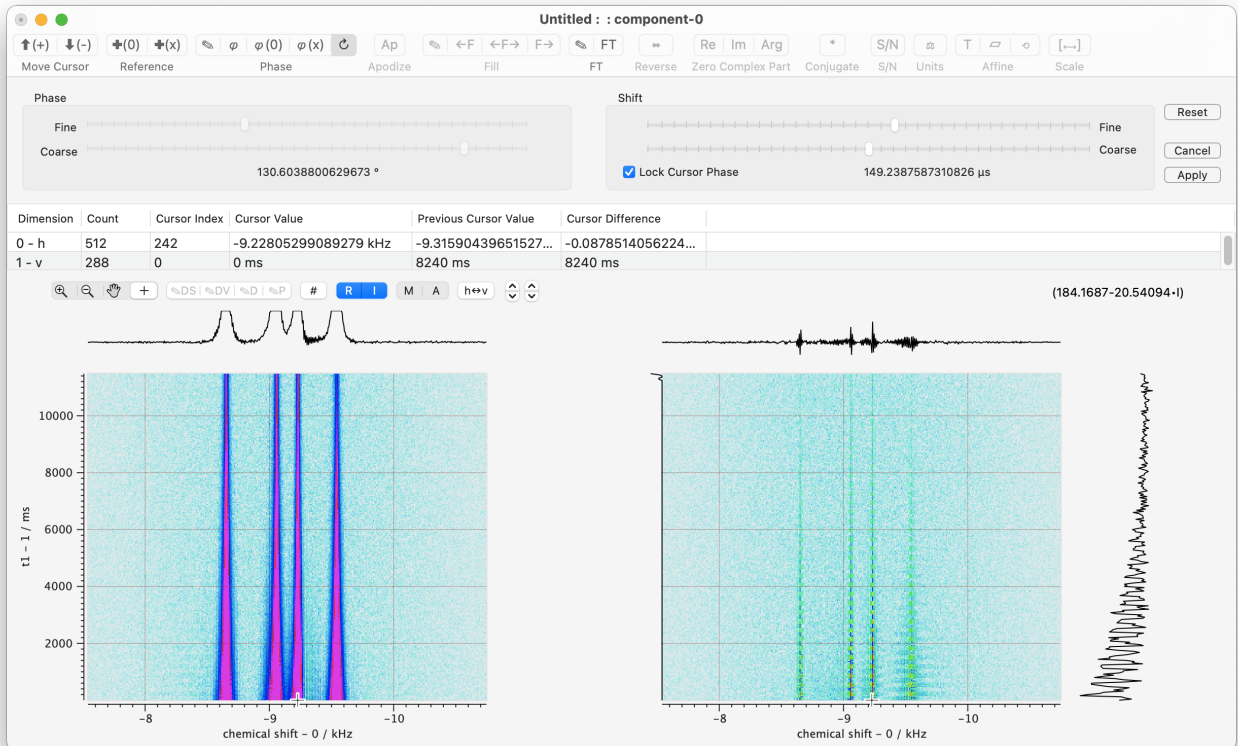
31. Move the cursor to the dependent variable maximum, i.e., up arrow in . We use this cursor position, at the highest intensity peak of the first t_1 cross-section (peak at 9.228 kHz), as the pivot point for applying an interactive phasing of the 2D signal. Open the Interactive Phasing, i.e., the in . Use the scroll wheel on the mouse to increase the intensity of the imaginary signal, as shown below.



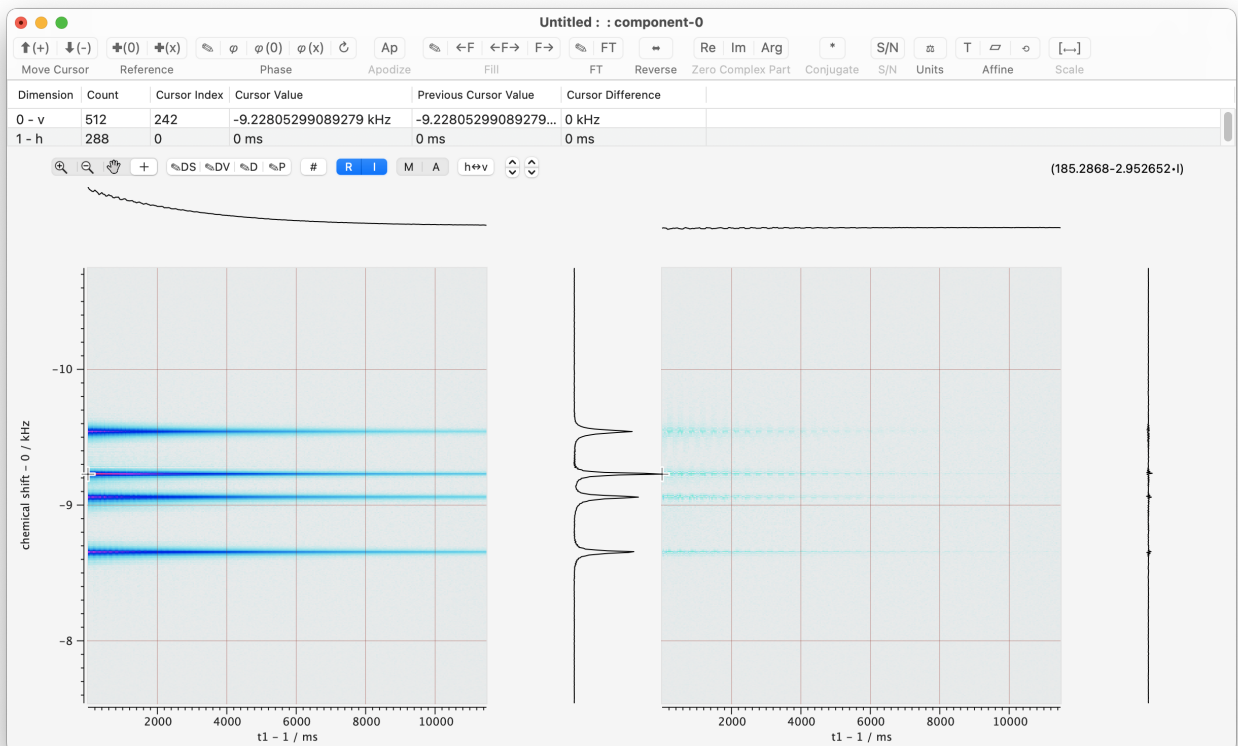
32. Adjust the zeroth order phase slider to make the peak at the cursor position, i.e., at 9.228 kHz, have the lowest intensity, as shown below.



33. Check the box to **lock the cursor phase** and adjust the first order phase slider to make all the peaks have the lowest intensity, and click on the Apply button on the right in the phase panel.

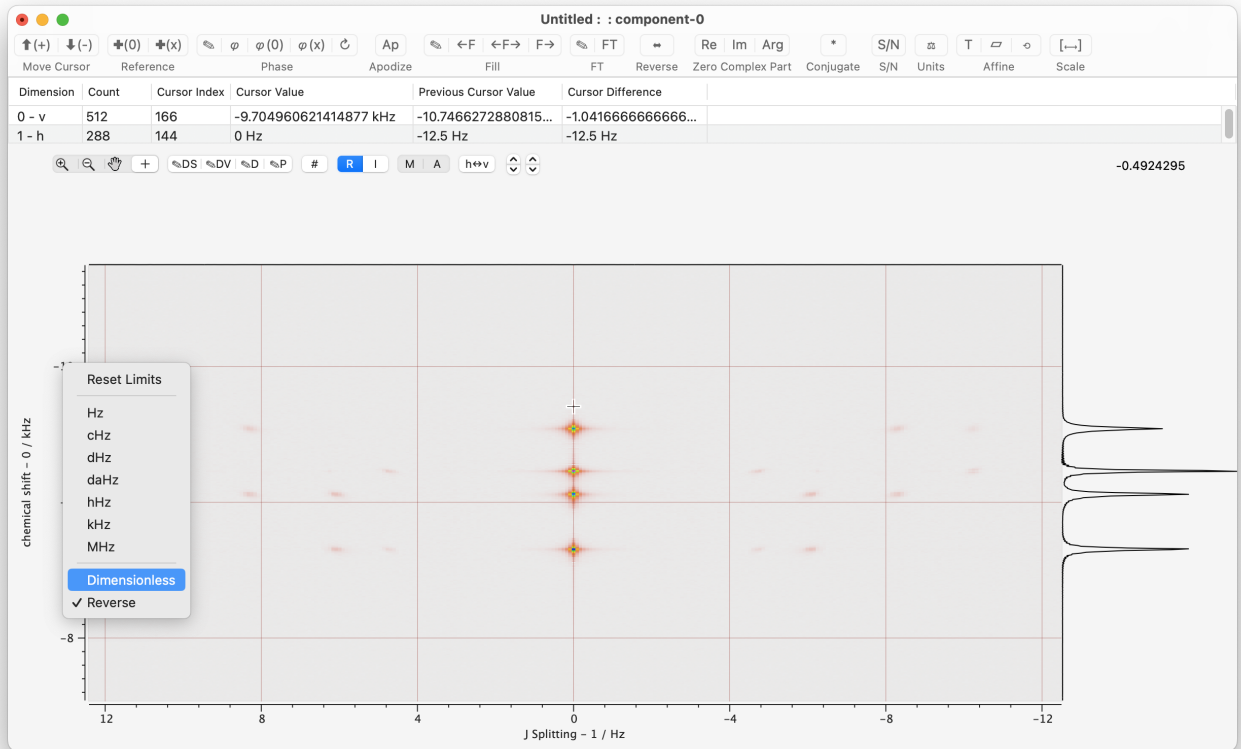


34. Unzoom, i.e., use the magnifying glass with the - in , and swap the horizontal/vertical dimension, i.e., use 

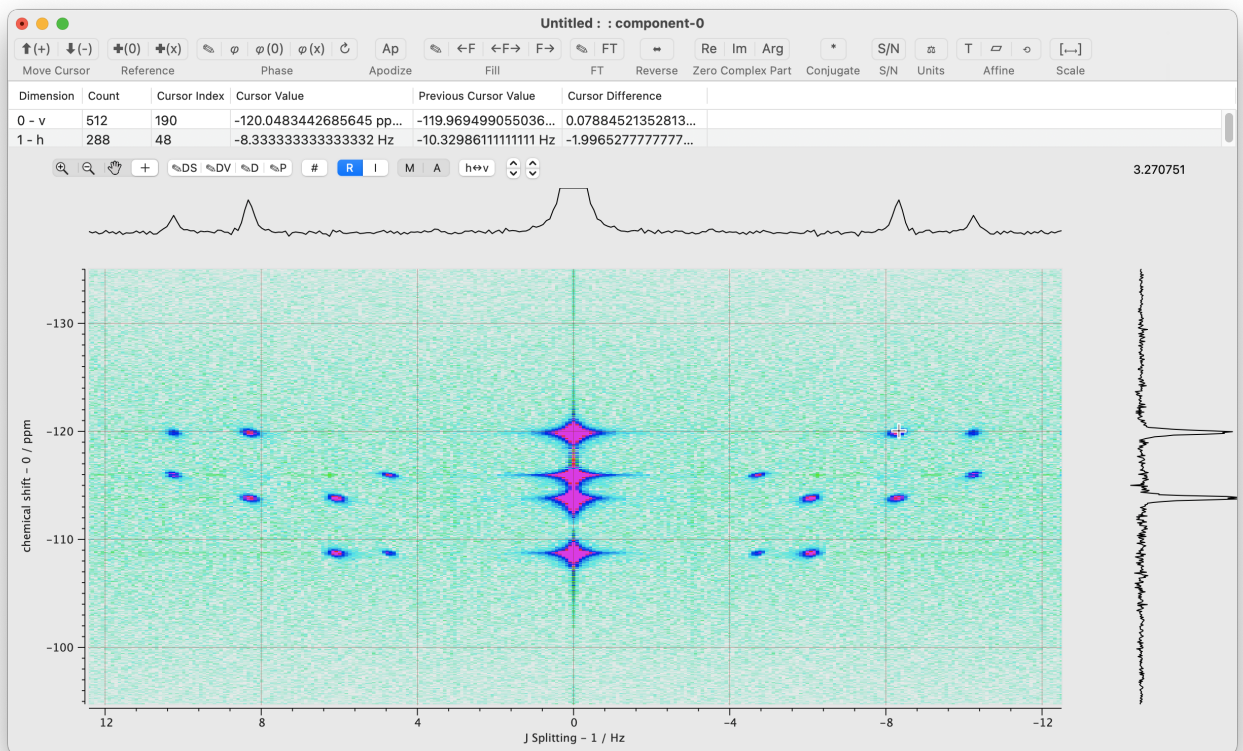


35. Under the **Process** menu go to the **Zero Complex Part** submenu and select **imaginary part of dataset**. Use command-F to apply a Fourier transform along the horizontal dimension.

36. Click on I in the **R I M A** to turn off the display of the imaginary part. Click on the vertical axis and select Dimensionless for the coordinate, as shown below.



37. Use the PageUp button on the keyboard to increase the intensity to see the *J* splittings as shown below.



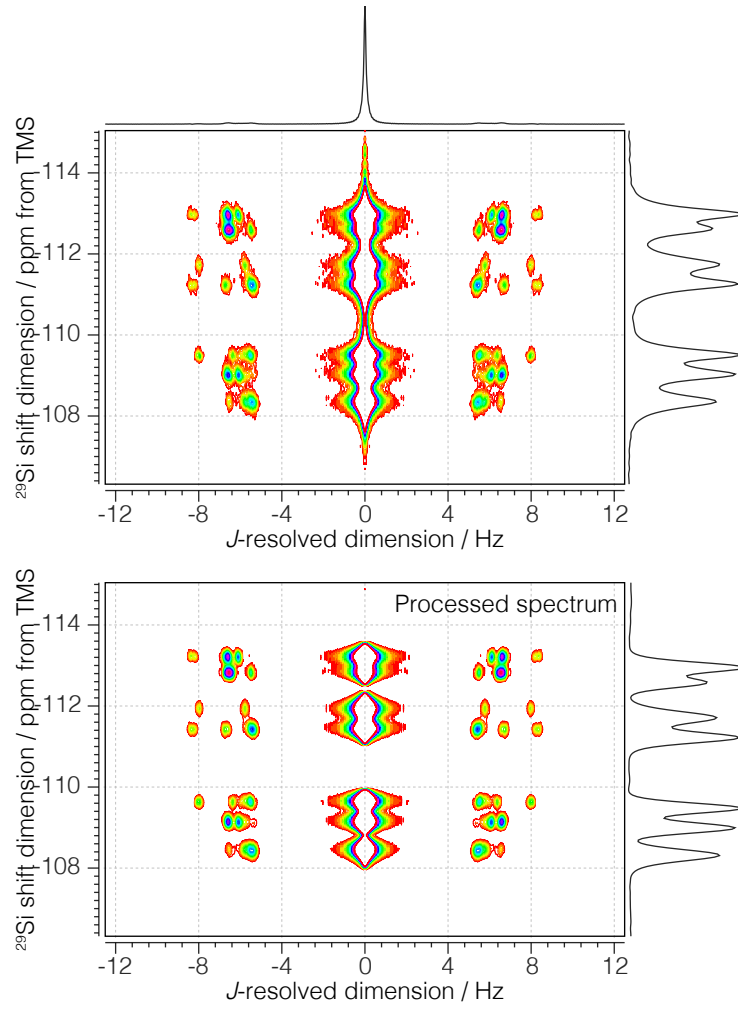


FIG. S6. (Top) The J -resolved SE-PIETA spectrum of ZSM-12. (Bottom) The processed spectrum was obtained by first apodizing the corresponding t_1 - t_2 signal with the function $\exp\left(\frac{|t_2|}{T_a}\right) \exp\left(-\frac{t_2^2}{2\sigma_a^2}\right)$ where $T_a = 16$ ms and $\sigma_a = 18$ ms. The apodizing signal was Fourier transformed and then further subjected to a noise reduction filter using singular value decomposition (SVD). The spectrum presented at the bottom was reconstructed after SVD by only retaining the first ten singular values.

S6. STRUCTURE REFINEMENTS

A. Optimization of Sigma-2

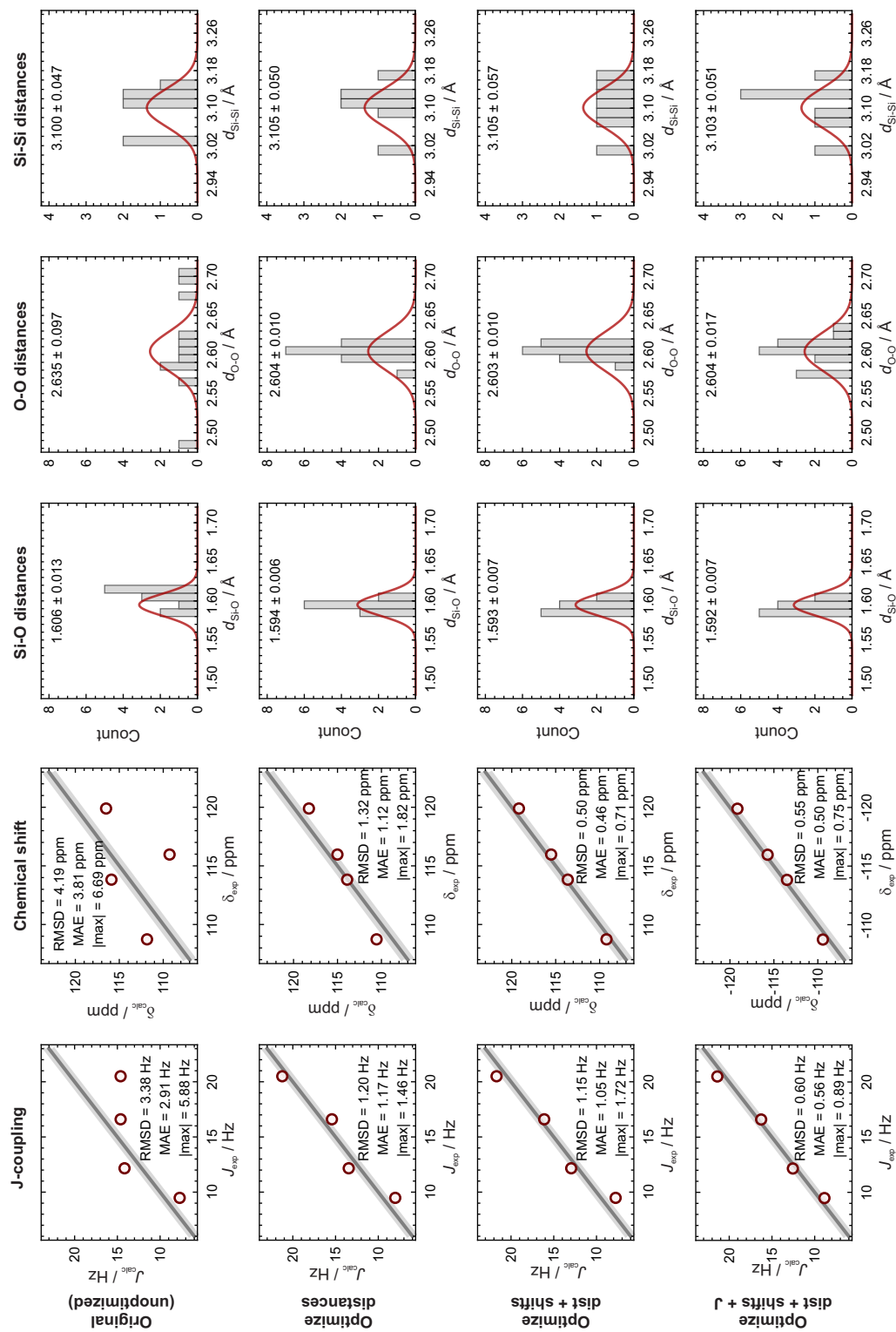


FIG. S7. Results of various optimizations for Sigma-2: original unoptimized structure derived from ^{29}Si double-quantum dipolar recoupling experiments (first row), after optimizing against distances only (second row), after full optimization against distances and chemical shifts (third row), after full optimization against distances, chemical shifts, and J-couplings (fourth row). The shaded bands in the J-coupling and chemical shift plots are $\pm s_J$ (0.58 Hz) and $\pm s_\delta$ (0.69 ppm). The red normal distributions with the distance histograms are the target distributions (as found in the analysis of SCXRD structures). The value above the histogram is the mean \pm standard deviation of the actual distances for the optimized structure.

cost function		Unoptimized	Optimize d	Optimize $d+\delta$	Optimize $d+\delta+J$
χ_d^2	$n_d = 34$	275.26	13.08	16.17	19.31
	χ_{SiO}^2 $n_{\text{SiO}} = 11$	14.87	1.90	2.44	3.05
	χ_{OO}^2 $n_{\text{OO}} = 16$	252.34	2.21	2.22	6.82
	χ_{SiSi}^2 $n_{\text{SiSi}} = 7$	8.04	8.97	11.51	9.43
χ_δ^2	$n_\delta = 4$	147.81	14.61	2.09	2.53
χ_J^2	$n_J = 4$	137.06	17.27	15.77	4.35
χ^2	$n = 42$	560.13	44.96	34.02	26.19
χ_ν^2	$\nu = 22$	13.34*	2.04	1.55	1.19

TABLE S1. Summary of various components of the cost function for Sigma-2 optimizations. Note that there are 20 fractional atomic coordinate parameters being refined, meaning there are $\nu = n - 20 = 42 - 20 = 22$ degrees of freedom. *For the original unoptimized structure in which there are no parameters being refined, the degrees of freedom used for calculating the reduced chi-square value χ_ν^2 is $\nu = n - 0 = 42$

Site	Experimental	Calculated Before Optimization		Calculated After Optimization		SCXRD Structure	
	$\delta_{\text{iso}}/\text{ppm}$	$\delta_{\text{iso}}/\text{ppm}$	$\Delta\delta_{\text{iso}}/\text{ppm}$	$\delta_{\text{iso}}/\text{ppm}$	$\Delta\delta_{\text{iso}}/\text{ppm}$	$\delta_{\text{iso}}/\text{ppm}$	$\Delta\delta_{\text{iso}}/\text{ppm}$
Si ₁	-115.97	-109.28	6.69	-115.71	0.26	-114.68	1.28
Si ₂	-113.82	-115.89	-2.07	-113.51	0.32	-113.38	0.44
Si ₃	-119.89	-116.50	3.39	-119.15	0.75	-118.34	1.56
Si ₄	-108.73	-111.84	-3.31	-109.43	-0.69	-108.73	-0.43
RMSD			4.19		0.55		1.06

TABLE S2. Comparison of experimental and calculated chemical shifts for Sigma-2 (before and after optimization against distances, chemical shifts, and J -couplings)

Site	Experimental	Calculated Before Optimization		Calculated After Optimization		SCXRD structure	
	${}^2J_{\text{Si-O-Si}}/\text{Hz}$	${}^2J_{\text{Si-O-Si}}/\text{Hz}$	$\Delta {}^2J_{\text{Si-O-Si}}/\text{Hz}$	${}^2J_{\text{Si-O-Si}}/\text{Hz}$	$\Delta {}^2J_{\text{Si-O-Si}}/\text{Hz}$		
Si ₂ -O ₂ -Si ₄	12.16	14.16	2.00	12.55	0.39	12.63	0.47
Si ₁ -O ₃ -Si ₃	20.50	14.62	-5.88	21.39	0.89	21.15	0.65
Si ₁ -O ₄ -Si ₄	9.48	7.71	-1.77	8.86	-0.62	6.63	-2.85
Si ₂ -O ₆ -Si ₃	16.60	14.62	-1.98	16.26	-0.34	15.09	-1.51
RMSD			3.38		0.56		1.37

TABLE S3. Comparison of experimental and calculated J -couplings for Sigma-2 (before and after optimization against distances, chemical shifts, and J -couplings)

Space group: $I 4_1/a m d : 2$ (#141)
 Cell parameters: $a = b = 10.2316 \text{ \AA}$, $c = 34.3642 \text{ \AA}$

Site	x	y	z
Si ₁	0.2858 (0.0014)	0.25	0.1180 (0.0007)
Si ₂	0.2831 (0.0023)	0	0
Si ₃	0.1531 (0.0012)	0.25	0.0347 (0.0006)
Si ₄	0.5	-0.0994 (0.0012)	0.0539 (0.0007)
O ₁	0.5	-0.25	0.0434 (0.0012)
O ₂	0.3727 (0.0012)	-0.0316 (0.0020)	0.0369 (0.0003)
O ₃	0.2287 (0.0036)	0.25	0.0753 (0.0007)
O ₄	0.5	-0.0780 (0.0013)	0.1000 (0.0006)
O ₅	0	0.25	0.0419 (0.0014)
O ₆	0.1948 (0.0017)	0.1228 (0.0009)	0.0106 (0.0005)

TABLE S4. Optimized fractional atomic coordinates (and estimated uncertainties) for Sigma-2.

B. Optimization of ZSM-12

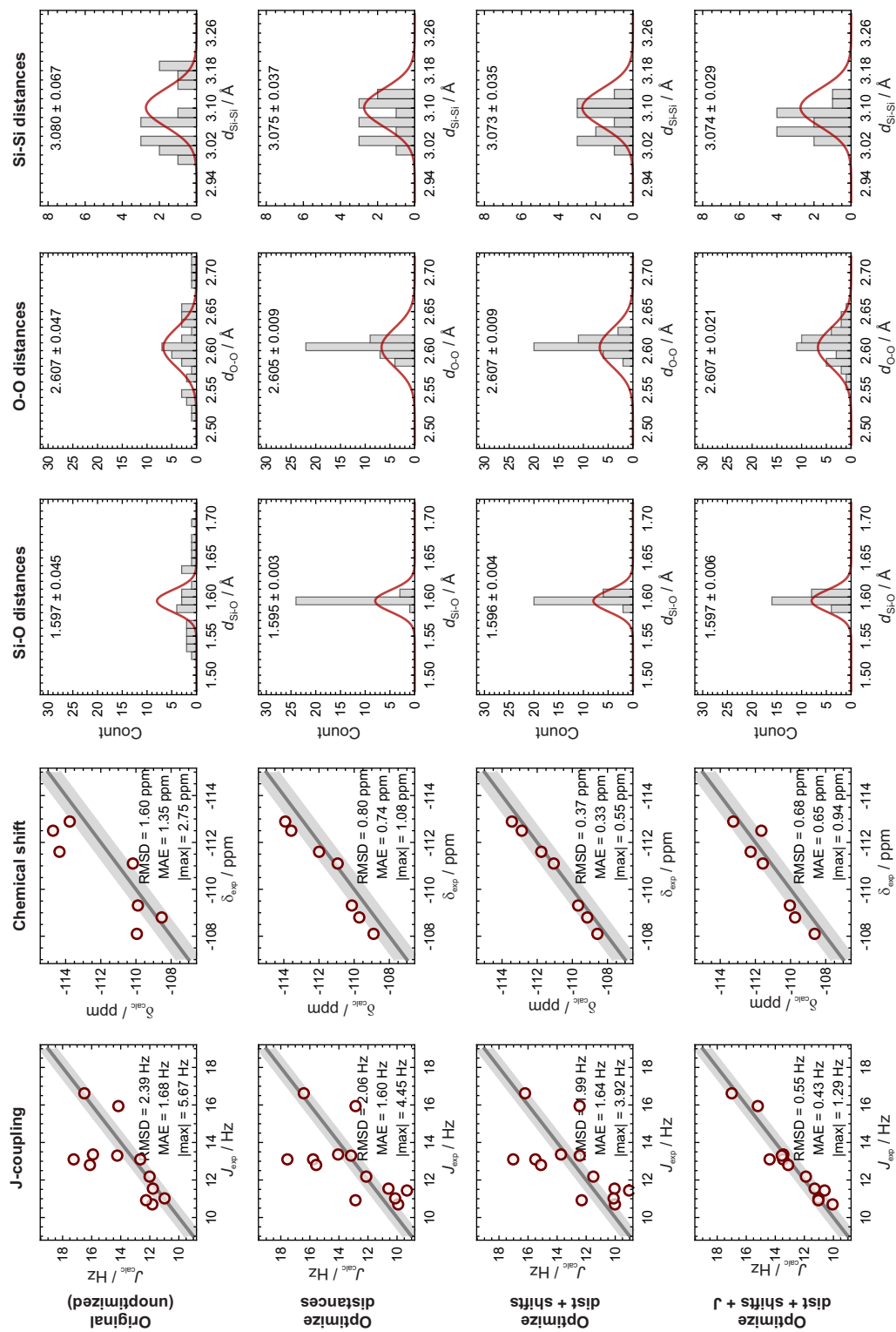


FIG. S8. Results of various optimizations for ZSM-12: original unoptimized structure (first row), after optimizing against distances only (second row), after optimizing against distances and chemical shifts (third row), after full optimization against distances, chemical shifts, and J-couplings (fourth row). The shaded bands in the J-coupling and chemical shift plots are $\pm s_J$ (0.58 Hz) and $\pm s_\delta$ (0.69 ppm). The red normal distributions with the distance histograms are the target distributions (as found in the analysis of SCXRD structures). The value above the histogram is the mean \pm standard deviation of the actual distances for the optimized structure.

cost function		Unoptimized	Optimize d	Optimize $d+\delta$	Optimize $d+\delta+J$
χ_d^2	$n_d = 84$	468.82	23.09	25.36	47.34
	χ_{SiO}^2 $n_{\text{SiO}} = 28$	283.69	1.44	2.82	5.04
	χ_{OO}^2 $n_{\text{OO}} = 42$	146.59	5.09	6.28	29.72
	χ_{SiSi}^2 $n_{\text{SiSi}} = 14$	38.54	16.55	16.27	12.59
χ_δ^2	$n_\delta = 7$	37.76	9.55	2.01	6.78
χ_J^2	$n_J = 13$	222.98	165.85	154.20	11.77
χ^2	$n = 104$	729.55	198.49	181.56	65.80
χ_ν^2	$\nu = 41$	7.01*	4.84	4.43	1.61

TABLE S5. Summary of various components of the cost function for ZSM-12 optimizations. Note that there are 63 fractional atomic coordinate parameters being refined, meaning there are $\nu = n - 63 = 104 - 63 = 41$ degrees of freedom. *For the original unoptimized structure in which there are no parameters being refined, the degrees of freedom used for calculating the reduced chi-square value χ_ν^2 is $\nu = n - 0 = 104$.

Site	Experimental	Calculated Before Optimization		Calculated After Optimization	
	$\delta_{\text{iso}}/\text{ppm}$	$\delta_{\text{iso}}/\text{ppm}$	$\Delta\delta_{\text{iso}}/\text{ppm}$	$\delta_{\text{iso}}/\text{ppm}$	$\Delta\delta_{\text{iso}}/\text{ppm}$
Si ₁	-111.10	-110.18	0.92	-111.59	-0.49
Si ₂	-112.89	-113.77	-0.88	-113.28	-0.39
Si ₃	-108.10	-109.95	-1.85	-108.65	-0.55
Si ₄	-108.80	-108.53	0.27	-109.75	-0.95
Si ₅	-112.50	-114.72	-2.22	-111.71	0.79
Si ₆	-109.31	-109.89	-0.58	-110.04	-0.73
Si ₇	-111.60	-114.35	-2.75	-112.26	-0.66
RMSD			1.60		0.68

TABLE S6. Comparison of experimental and calculated chemical shifts for ZSM-12 (before and after optimization)

Site	Experimental	Calculated Before Optimization		Calculated After Optimization	
	${}^2J_{\text{Si-O-Si}}/\text{Hz}$	${}^2J_{\text{Si-O-Si}}/\text{Hz}$	$\Delta {}^2J_{\text{Si-O-Si}}/\text{Hz}$	${}^2J_{\text{Si-O-Si}}/\text{Hz}$	$\Delta {}^2J_{\text{Si-O-Si}}/\text{Hz}$
Si ₁ -O ₁ -Si ₂	16.62	16.50	-0.12	17.00	0.38
Si ₁ -O ₂ -Si ₂	13.36	15.91	2.55	13.44	0.08
Si ₁ -O ₃ -Si ₃	10.70	11.83	1.13	10.01	-0.69
Si ₃ -O ₄ -Si ₅	13.10	17.24	4.14	14.44	1.34
Si ₂ -O ₅ -Si ₄	13.10	12.65	-0.45	13.47	0.37
Si ₃ -O ₆ -Si ₇	11.54	11.79	0.25	11.26	-0.28
Si ₅ -O ₈ -Si ₆	12.80	16.12	3.32	13.13	0.33
Si ₄ -O ₉ -Si ₆	11.44	5.77	-5.67	10.54	-0.90
Si ₄ -O ₁₀ -Si ₅	13.30	14.24	0.94	13.56	0.26
Si ₆ -O ₁₁ -Si ₇	15.94	14.16	-1.78	15.16	-0.78
Si ₁ -O ₁₂ -Si ₃	11.02	10.98	-0.04	11.02	-0.00
Si ₂ -O ₁₃ -Si ₄	12.18	12.01	-0.17	11.87	-0.31
Si ₅ -O ₁₄ -Si ₆	10.92	12.25	1.33	11.03	0.11
RMSD			2.39		0.55

TABLE S7. Comparison of experimental and calculated J -couplings for ZSM-12 (before and after optimization)

Space group: $C 2/c$ (#15)
 Cell parameters: $a = 24.8633 \text{ \AA}$, $b = 5.01238 \text{ \AA}$, $c = 24.3275 \text{ \AA}$, $\beta = 107.722^\circ$

Site	x	y	z
Si1	0.0593 (0.0009)	0.0355 (0.0076)	0.0856 (0.0009)
Si2	0.4311 (0.0010)	0.4270 (0.0065)	0.0396 (0.0011)
Si3	0.3753 (0.0009)	0.0344 (0.0076)	0.3627 (0.0010)
Si4	0.1356 (0.0010)	0.4245 (0.0064)	0.4486 (0.0010)
Si5	0.2847 (0.0010)	0.0807 (0.0071)	0.4258 (0.0011)
Si6	0.2856 (0.0010)	0.0838 (0.0070)	0.1197 (0.0009)
Si7	0.2849 (0.0006)	-0.0009 (0.0115)	0.2459 (0.0008)
O1	0.0728 (0.0012)	0.0206 (0.0086)	0.0260 (0.0010)
O2	0.4951 (0.0010)	0.4673 (0.0080)	0.0789 (0.0008)
O3	0.0741 (0.0009)	0.3258 (0.0082)	0.1136 (0.0015)
O4	0.1682 (0.0013)	0.4827 (0.0065)	0.1021 (0.0014)
O5	0.4121 (0.0012)	0.1283 (0.0065)	0.0476 (0.0020)
O6	0.1562 (0.0007)	0.4782 (0.0096)	0.2041 (0.0009)
O7	0.2456 (0.0021)	0.2148 (0.0154)	0.2628 (0.0013)
O8	0.2646 (0.0010)	0.3789 (0.0073)	0.4082 (0.0017)
O9	0.3409 (0.0009)	-0.0048 (0.0079)	0.1040 (0.0008)
O10	0.3115 (0.0010)	0.0626 (0.0091)	0.4945 (0.0010)
O11	0.2966 (0.0013)	0.0836 (0.0095)	0.1875 (0.0008)
O12	0.3998 (0.0014)	0.3286 (0.0082)	0.3708 (0.0011)
O13	0.1093 (0.0014)	0.1309 (0.0069)	0.4410 (0.0016)
O14	0.2675 (0.0010)	0.3765 (0.0077)	0.0946 (0.0018)

TABLE S8. Optimized fractional atomic coordinates (and estimated uncertainties) for ZSM-12.

Additional Supporting Information files in SuppInfoFiles.zip

- Mathematica notebook “ZeoliteRefinement-final.nb”
- .cif files of optimized structures:
 - MTW-Fyfe-1990.cif
 - MTW-Fyfe-1990-dist.cif
 - MTW-Fyfe-1990-dist+shifts.cif
 - MTW-Fyfe-1990-dist+shifts+J.cif
 - SGT-Brouwer-2008-NMR.cif
 - SGT-Brouwer-2008-NMR-dist.cif
 - SGT-Brouwer-2008-NMR-dist+shifts.cif
 - SGT-Brouwer-2008-NMR-dist+shifts+J.cif
- Data used for parameterizations:
 - “shift-structure-SCXRD.txt” = Chemical shift and local geometry data
 - “clusterJcouplings.txt” = J -coupling data

-
- [1] P. J. Grandinetti, J. T. Ash, and N. M. Trease, Prog. Nucl. Mag. Res. Sp. **59**, 121 (2011).
[2] G. Bodenhausen, H. Kogler, and R. R. Ernst, J. Magn. Reson. **58**, 370 (1984).
[3] D. J. Srivastava and P. J. Grandinetti, J. Chem. Phys. **160** (2024), 10.1063/5.0209887.
[4] D. Srivastava, J. Baltisberger, P. Florian, F. Fayon, R. Shakhovoy, M. Deschamps, N. Sadiki, and P. Grandinetti, Phys. Rev. B **98**, 134202 (2018).
[5] PhySy Ltd., “RMN 2.0,” (2019).